BEHAVIOR OF EXTENDED SHEAR TABS IN STIFFENED

BEAM-TO-COLUMN WEB CONNECTIONS

By

Warren Goodrich

Thesis

Submitted to the Faculty of the

Graduate School of Vanderbilt University

in partial fulfillment of the requirements

for the degree of

MASTER OF SCIENCE

in

Civil Engineering

August, 2005

Nashville, Tennessee

Approved:

Dr. P.K. Basu

Dr. Lori Troxel

For my wonderful parents, Scott and Brent, who gave me every opportunity to succeed

and

For my beloved wife, Elisa, infinitely supportive

ACKNOWLEDGEMENTS

TABLE OF CONTENTS

Page

Chapter

LIST OF TABLES

LIST OF FIGURES

ix

LIST OF ABBREVIATIONS

AISC .... American Institute of Steel Construction

ASCE .... American Society of Civil Engineers

C .... Compression (force)

CL .... Centerline

EST .... Extended Shear Tab

FEM .... Finite Element Modeling

FS .... Factor of Safety

HPCL .... High-Performance Computer Laboratories

LRFD .... Load and Resistance Factor Design

SSL .... Short-Slotted (Holes)

STD .... Standard (Holes)

T .... Tension (force)

App. .... Appendix

Fig. .... Figure

CHAPTER I

INTRODUCTION

Extended Shear Tabs

In steel-frame buildings, connections are used to transmit loads from beams to girders and from both beams and girders to columns. The connections consist of connecting elements like plates, angles, tees, etc., and fasteners like bolts and welds. Depending upon the type of connection used, it may be termed as fully rigid, semi-rigid or simple. Fully rigid connections provide full moment continuity at the joint, whereas a simple connection transmits shear only, developing no moment at the joint. Typical examples of rigid, semi-rigid, and common simple connections are shown in Figure 1.
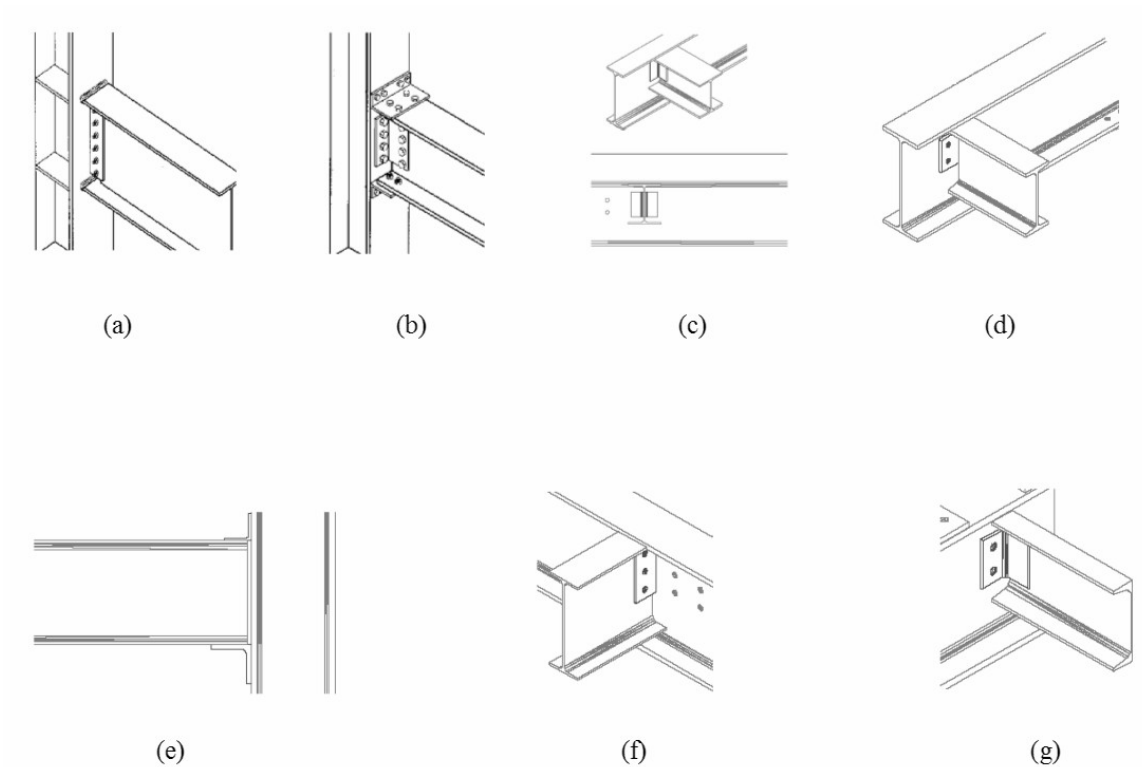
Figure 1: Illustrations of typical steel connections; (a) is a fully rigid connection; (b) is a semi-rigid connection; (c) – (g) are simple connections

Still, the designations of connection types are not true reflections of the behavior. As shown in Figure 2, neither the rigid connections nor the simple connections are exact representations of connection-type assumptions. However, the design procedures developed for most of these connection types lead to safe connections. It may be noted that before a structure can be analyzed it is necessary to make an assumption of the connection types. The forces created in the structural elements are affected by this choice. Thereafter, it is necessary to design the connections using the member end forces obtained, and it is imperative that the behavior of the chosen connections is consistent with the original assumptions.

End Moment, M

$\frac{Pu*L}{8}$

Fully rigid support

Semi-rigid support

Simple support

End Rotation, Θ

1/2 * Fy/E * L/d
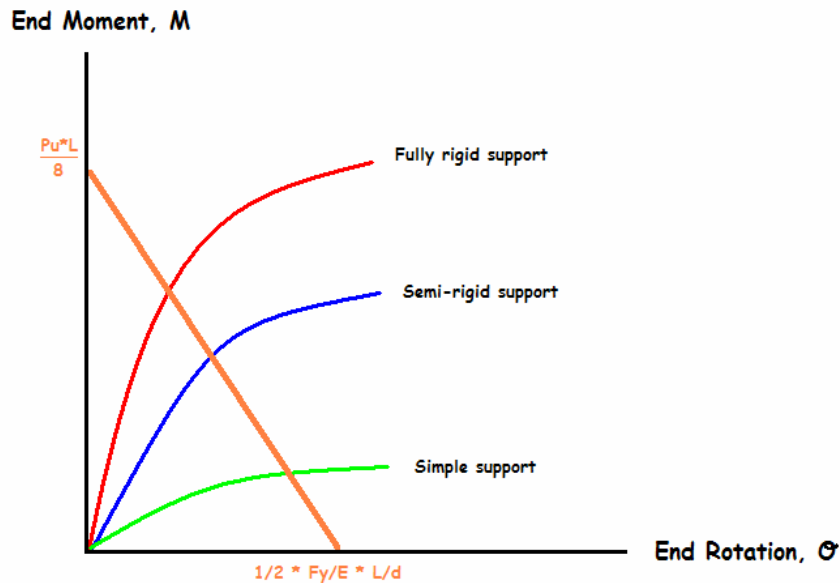
Figure 2: Typical moment-rotation curves for different connection types (point load P_u at center)

Simple (shear) connections are most commonly used in beam/girder to column connections or beam to girder connections. Some examples of such connections, shown, respectively, in Figure 1 (c) to (g) are double angle, shear end plate, unstiffened seated, single plate, and single angle. Of these, the single plate connection, or shear tab, is popular due to ease in fabrication and erection, superior strength, and cost efficiency. As shown in Figure 3, the shear tab connection typically consists of a plate that is shop-welded to the supporting member (say, a column) and then field-bolted to the supported member (say, a beam).

2

One such configuration involves a beam framing into the web of a column that has moment connections on its flanges. This type of connection to the column's strong axis is typically found in a rigid frame. It utilizes continuity plates to reinforce the continuous nature of the connection and to stabilize the column flanges (see Figure 3). In this case, the shear tabs for the beams that frame into the column's weak axis are welded to the column web between the continuity plates. However, the continuity plates interfere with the beams such that a direct connection to the column web cannot be made without coping the beam. For many fabricators, it is more cost-efficient to make a shear tab connection that extends beyond the continuity plates than to cope the beam in this situation.
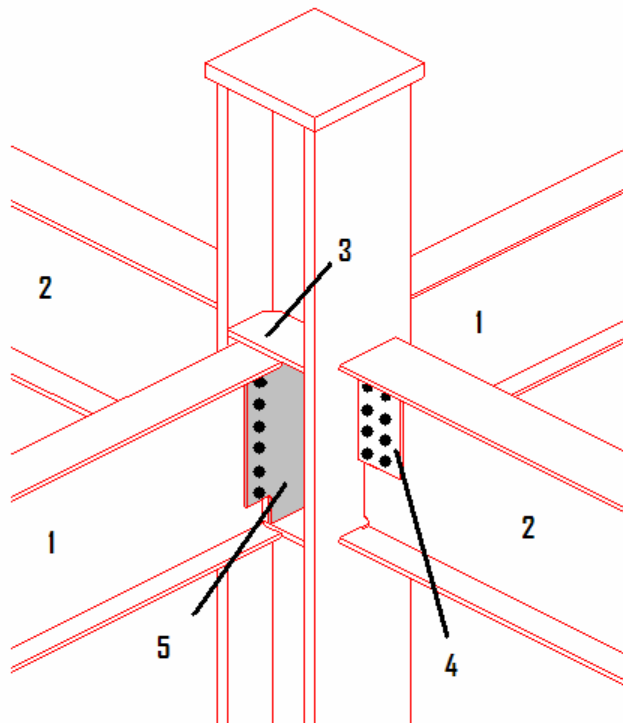
1. Beams that frame into the column web
2. Beams that frame into the column flanges
3. Top continuity plate for the moment connections
4. Standard shear tab for moment connection
5. Extended shear tab (to be analyzed)

Figure 3: Extended shear tab used to connect a beam to a column's weak axis
instead of coping the beam and using a standard shear tab

Two possible shear tabs are shown in Figure 3. The connection of the strong-axis beam to the column flange utilizes a standard shear tab connection while the connection of the weak-axis beam to the column web utilizes an extended shear tab (EST) connection. The current American Institute of Steel Construction (AISC) Manual of Steel Construction by the Load and Resistance Factor Design (LRFD) method, Third Edition (the "Manual"), gives a design procedure on page 10-112 for standard shear tab connections. There is one limitation that states that the distance "a" between the centroid of the bolt line to the centroid of the weld pattern should satisfy the condition 2 ½" $\leq$ a $\leq$ 3 ½" (see Figure 4).
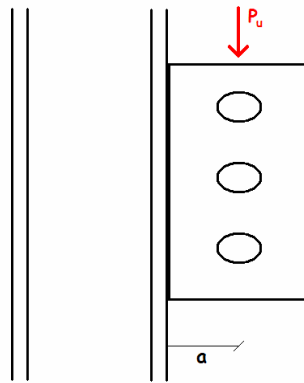
Figure 4: Standard shear tab connection

On page 10-117 the Manual, Table 10-9 contains a collection of design tables for two cases depending upon the relative stiffness of the supporting member: a) flexible support and b) rigid support. In both cases, the bolt line is designed for a direct shear effect of P_u and a torque equal to $P_u * e_b$. The values for e_b are described below (n = number of bolts).

For both flexible and rigid supports with standard bolt holes,

$$e_b = |(n-1) - a| \tag{1}$$

For both flexible and rigid supports with short-slotted holes,

$$e_b = |2/3 * n - a| \tag{2}$$

Flexible supports must meet a minimum requirement,

$$e_b \geq a \tag{3}$$

There is no provision for extended plate connections in the Manual except the statement "single-plate connections with geometries and configurations other than those described above can be used based upon rational analysis" (p. 10-113). The use of extended shear tabs in column web connections makes erection easier and fabrication less expensive. Additionally, in a beam-to-girder connection, extending the plate often eliminates the need to cope the top flange of the beam. As can be seen in Figure 5, the result is an increase in "a" to a value above 3 ½", which is outside the AISC limits specified for standard shear tab connections.
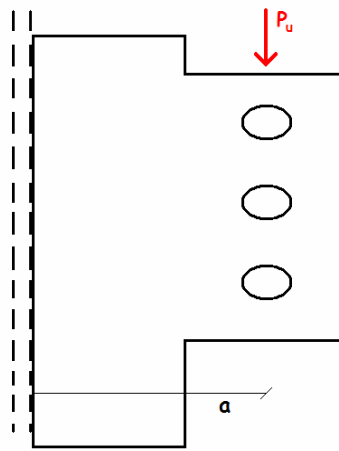
Figure 5: Extended shear tab connection

Many investigators contend that when the EST is stiffened by continuity plates, they stabilize the shear tab and pick up some of the load, allowing the effective eccentricity to be reduced. This reduction may create a larger moment in the column, but often the column would be strong enough to handle this extra moment. The effects of extended shear tabs on the column are not considered in this study. One of the primary goals of this study is to determine the role of the continuity plates in the connection, and the other goal is to determine if a design based on reduced eccentricity will be safe. The objectives of this study can be stated as follows.

1. Review the current practice of shear tab design and identify any limitations

2. Propose a method of design of extended shear tabs for this framing situation

3. Design three typical connections based on the proposed method of step 2

4. Fabricate full-scale test specimens, each consisting of a beam, column, and extended shear tab connection

5. Test the full-scale specimens to determine the connections' behavior up to the limit state

6. Undertake nonlinear finite element modeling (FEM) of appropriate segments of the specimens

7. Evaluate the test data, finite element predictions, and proposed design method

8. Draw conclusions and make recommendations

Chapter I has covered the introduction, stated general objectives, and will review past work. Chapter II involves the fabrication and mechanics of the connection in a thorough manner. Chapter III details the proposed design method and applies it to design the test specimens. Chapter IV includes the experimental investigation while Chapter V deals with the finite element analysis of the connection. Chapter VI compares the testing, analysis and design results, states conclusions and makes recommendations.

Review of Past Work

Shear tabs have been a popular connection for over 30 years, but the investigation of extended shear tabs is a much younger topic. Many researchers and professionals have studied extended shear tabs, but the results have been such that no definitive design procedure has been reached. There are so many different types of framing conditions where extended shear tabs could be used that it is very difficult for a design procedure to encompass all of the cases. Some of the more notable research on this topic has been performed by Professor Ralph Richard of the University of Arizona (Ref: Richard, et al.), Professor Abolhassen Astaneh of the University of California at Berkeley (Ref: Astaneh, et al.), and Drs. Don Sherman and Al Ghorbanpoor of the University of Wisconsin-Milwaukee (Ref: Sherman and Ghorbanpoor). Richard's work dealt mostly with the development of standard shear tabs and is really the foundation for the design procedure used in the current Manual. The work of Astaneh and of Sherman and Ghorbanpoor dealt with extended shear tabs, but the results of their research led to a clearer understanding of the mechanics involved and other original design procedures, for the most part unrelated to the

hypothesis of this project. Mr. Tom Ferrell and Mr. David Rutledge of Ferrell Engineering, along with Mr. Chris Hewitt of AISC, have been recently working on a Design Guide for Extended Shear Tabs. A preliminary version of the Guide (Ref: Ferrell, et al.) covered the configuration studied in this project, but it was clear that the hypothesis of this project was neither proven nor disproven in the Guide.

Although there has never been a project with a hypothesis similar to this one, some valuable information can be taken from past research. The research of Drs. Sherman and Ghorbanpoor produced a lot of experimental data based on tests of many different configurations. Also, much was learned from their testing procedure and implemented in the testing phase of this project. Some of the relevant conclusions taken from their experimental work are listed below:

- The vertical weld from the tab to the column web is required

- Stiffener plates do not need to be welded to the column web if the tab is welded to the column web

- The overall length of the tab should not exceed twice the length of the extended part

- Stiffener plates can carry over 40% of the shear force at the connection

The preliminary version of the Design Guide showed what is likely to become the latest procedure for design of extended shear tabs upon its official release, but it is not being currently used by designers. The design procedure developed in the Guide arbitrarily devotes 5% of the weak axis column flexural strength to the moment caused by the extended shear tab. However, it fails to provide a detailed procedure for the design of the extended shear tab itself. After viewing the past research, it was determined that investigation of this project and its hypothesis was both viable and valuable for the industry.

CHAPTER II

FABRICATION AND MECHANICS OF THE CONNECTION

Fabrication of the Connection

The following list is a step-by-step procedure to fabricate an extended shear tab connection. Illustrations following the list may help to clarify the procedure.

1. The column should be resting on its back

2. Tack weld all 3 plates to their proper locations (tack welds are not supporting welds, they are just spot welds to hold the plates in position while applying the supporting welds)

3. Weld one continuity plate to the web of the column on both sides of the plate

4. Weld the other continuity plate to the web of the column on both sides of the plate

5. Weld the shear tab to the web of the column on both sides of the tab

6. Turn the column over on its side so it is resting on one flange

7. From the top position, weld one continuity plate to the bottom flange

8. Repeat with the other continuity plate to the bottom flange

9. Weld the tab to one continuity plate, then the other

10. Rotate the column onto its other flange

11. From the top position again, weld one continuity plate to the bottom flange

12. Repeat with the other continuity plate to the bottom flange

13. Weld the tab to one continuity plate, then the other

All welds from the continuity plates to the column are full-penetration welds and all welds from the tab to the continuity plates are groove welds.
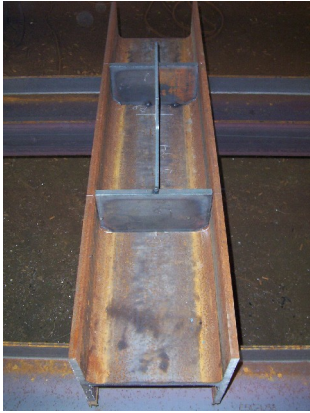
Figure 6: (Steps 1-2) Place column on its back and tack weld the plates
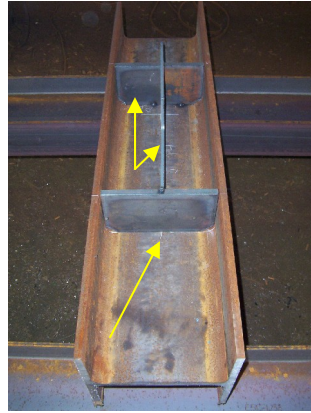
Figure 7: (Steps 3-5) Weld at the above locations and other similar locations

Figure 8: (Steps 6-9 and 10-13) Turn the column onto its flange and weld at the above locations and other similar locations

Failure Mechanisms and Limit States

There are several limit states that are to be checked in the design of extended shear tabs. The following outline lists the limit states and how they are defined and designed in the Manual. For a detailed example of the design of an extended shear tab analyzing all of the following limit states, see Appendix A.

A. BOLTS IN SHEAR WITH ECCENTRIC LOADING

Table 7-10 gives design strength per bolt; for ¾" A325-N the design strength is $\Phi * r_n$ = 15.9 kips

Table 7-17 gives C to determine the design strength of a single vertical row of bolts

Table 7-18 gives C to determine the design strength of two vertical rows of bolts

B. SUPPORTED BEAM WEB

Table 10-1 gives the design strength of the beam web per inch thickness

C. SHEAR RUPTURE OF THE SHEAR TAB

The design strength is found on page 16.1-67 of the Specification of the Manual ("the Specification")

9

D. BLOCK SHEAR RUPTURE OF THE SHEAR TAB

The design strength is found on page 16.1-67 of the Specification

E. HORIZONTAL BUCKLING OF THE SHEAR TAB NEAR THE COPE

The design strength is found on page 16.1-27 of the Specification

F. HORIZONTAL YIELDING OF THE SHEAR TAB NEAR THE COPE

The design strength is found on page 16.1-68 of the Specification

G. BEARING STRENGTH ON THE BOLT HOLES

The design strength is found on page 16.1-66 of the Specification

H. FLEXURE STRENGTH OF CONTINUITY PLATES

The design strength is found on page 16.1-31 of the Specification

J. TENSILE STRENGTH OF CONTINUITY PLATES

The design strength is found on page 16.1-24 of the Specification

K. COMPRESSIVE STRENGTH OF CONTINUITY PLATES

The design strength is found on page 16.1-27 of the Specification

L. WELDS IN SHEAR

Table 8-4 gives the coefficient C_1 for the electrode size

Table 8-9 gives the coefficient C for the weld geometry and load eccentricity

Table 8-9 also gives the design size of the weld, D, for the weld geometry and load eccentricity

M. SHEAR YIELDING OF THE SHEAR TAB

The design strength is found on page 16.1-68 of the Specification

CHAPTER III

SIMPLIFIED DESIGN PROCEDURE

The extended nature of the shear tab is critical due to the fact that it induces a larger moment in the plate. The load is transferred from the beam to the column through the bolts and welds, but the load from the beam is at the centroid of the bolts and the load to the column is at the centroid of the weld pattern. Since these two locations are not coincident, the larger eccentricity causes a larger moment. However, when the shear tab is stiffened by the continuity plates, it is reasonable to assume that the load is transferred to the column by a combination of both the shear tab and the continuity plates, reducing the eccentricity.

A possible design procedure is simply that extended shear tabs in this framing situation can be designed using the design tables in Table 10-9 of the Manual. By allowing use of Table 10-9, it is implied that the value of "a" has been effectively reduced to be within the range $2\frac{1}{2}$" $\leq$ a $\leq$ $3\frac{1}{2}$". This proposed method requires that the continuity plates be sufficient to carry a large portion of the load. The common practice is that the size of the continuity plates is determined by the thickness of the flanges of the strong-axis beams. These beams are usually heavy members, since they are part of a rigid frame, so the continuity plate thickness is normally at least ¾". However, they should meet at least a minimum requirement based on the load at the connection. Since the shear tab is designed as a function of the reaction, the continuity plate can be designed as a function of the shear tab thickness. Based on a mechanics analysis shown in Appendix A, as a minimum they should be 1.5-times the thickness of the shear tab that is designed using Table 10-9 of the Manual. The welds that fix the continuity plates to the column are also critical and are normally 75% of the thickness of the continuity plates. However, as a minimum, they should be 1.5-times the thickness of the welds of the shear tab that are designed using Table 10-9 of the Manual. A summary of the three points of the design procedure is listed below.

- The thickness of the shear tab plate, the number of bolts, and the thickness of the shear tab welds are determined using the standard shear tab design tables, Table 10-9 of the Manual

- The continuity plate thickness matches the strong-axis beam flange thickness and has a minimum value of 1.5-times the shear tab thickness

11

- The thickness of the continuity plate welds equals 75% of the thickness of the continuity plates and has a minimum value of twice the thickness of the shear tab welds

The application of this procedure for the following two connections is discussed in the following chapters.

1. Reaction = 44.7 kips

    a. Table 10-9 gives a 3/8" shear tab with four holes and 5/16" welds

    b. Continuity plate thickness must be at least 9/16"

    c. Continuity plate welds must be at least 1/2"

2. Reaction = 27.8 kips

    a. Table 10-9 gives a 1/4" shear tab with three holes and 3/16" welds

    b. Continuity plate thickness must be at least 3/8"

    c. Continuity plate welds must be at least 5/16"

CHAPTER IV

EXPERIMENTAL INVESTIGATION

Overview of the Testing Program

Experimental investigation was planned for a clear understanding of extended shear tab connections, as well as for validating computer simulations and the design procedure used to proportion the connections. For these purposes, it was necessary to measure strains (or stresses) and deformations at critical locations of the connections.

A series of six tests were conducted. There were three different testing sessions and each session had two tests each. The two connection details within each session were identical, but the details varied from session to session. The test setup simulated a 30-foot long simply supported beam (W27x84) with a uniformly distributed load and extended shear tab connections at the ends. This was accomplished by providing the connection at one end only; the other end was simply supported. The load was applied as a point load, but the location of the point load was chosen so the end reaction and rotation were the same as created by a uniformly loaded beam. Appendix B shows the analysis used to determine the location of the point load. This loading strategy allowed creation of larger shear in the connection without the need for applying a load that is twice the shear value. For the sake of savings in time and economy, the same beam was used for all of the tests. In each testing session, the beam was connected to the web of a five-foot column using an extended shear tab connection. The column had continuity plates and shear tabs welded on each side of the web. The beam had standard round holes punched in each end to connect to the short slotted holes (SSL) of the shear tab. Both sides of the column web and both ends of the beam were identical.

After the first test of each session, both the beam and the column were flipped over, and the connection at the other end of the beam was properly made. Then the second test was run. After each session, a new column stub was fabricated and six inches was cut off each end of the beam so that the deformed holes were removed. Thereafter, new holes were drilled for the next test. Since the flexure stress in the beam never reached its yield point, the beam never experienced any plastic deformation. The only

possibility for plastic deformation was at the beam holes, but because six inches was cut off the end after each session, those stresses were removed before the next test. Thus, after the ends were cut and new holes were drilled, the beam was free of residual stresses and ready for the next testing session.

Table 1 gives details of the test setup for each of the three sessions.

Table 1: Information for each testing session

SESSION	SESSION 1	SESSION 2	SESSION 3
Factored end reaction for design	44.7	27.8	27.8
Strong-axis beam	W24x84	W16x77	W16x77
Column size	W14x99	W14x99	W14x99
Weak-axis beam	W27x84	W27x84	W27x84
# of holes and hole type	4 - SSL	3 - SSL	3 - SSL
Effective height of tab	12"	9"	9"
Overall height of tab	22.56"	14.98"	14.98"
Thickness of tab	⅜"	¼"	½"
Predicted beam deflection Δ_{max}	0.234"	0.157"	0.146"
Predicted end rotation θ_{max}	0.184°	0.113°	0.107°
Size of tab welds	5/16"	3/16"	5/16"
Size of cont. plate welds	9/16"	9/16"	9/16"
Cont. plate thickness	¾"	¾"	¾"
Bolt size and type	¾" A325-N	¾" A325-N	¾" A325-N
Rigid or flexible support	Flexible	Flexible	Flexible
Unsupported length of test beam	29'	28'	27'
Dist. from load to end of beam	6'	6'	6'
Point load to cause design reaction	50 kips	35 kips	36 kips

Notes for Table 1

- The factored end reaction was chosen to exactly match a value from Table 10-9; the connections were designed based on this load in accordance with the Manual. (App. E)

- The strong-axis beam was chosen to represent a likely scenario based on load; this beam was not part of the tests, but the connection would have been a moment connection, as in a rigid frame.

- The column size was chosen based on availability and is a common size in rigid frames.

14

- The weak-axis beam was chosen based on availability and strength requirements (so the same beam could be used for all tests – App. C).

- The number of holes was determined in designing the shear tab using Table 10-9 of the Manual.

- The effective height of the tab is the extended part and was based on the number of holes and bolt spacing, 3" c/c.

- The overall height of the tab was the clear distance between the continuity plates, whose locations in the column match the flanges of the strong-axis beams on the column flanges.

- The thickness of the tab was determined in designing the shear tab using Table 10-9.

- The predicted beam deflection was determined using standard deflection equations. (App. D)

- The predicted beam end rotation was determined using standard rotation equations. (App. D)

- The thickness of the tab welds was determined in designing the shear tab using Table 10-9.

- The continuity plate thickness matched the thickness of the flanges of the strong-axis beam; it has a minimum value of 1.5-times the thickness of the tab welds.

- The thickness of the continuity plate welds was based on the size of the strong-axis beam.

- The bolt size and type were determined in designing the shear tab using Table 10-9.

- Flexible support was used because the column was unfixed; this support condition affected the design using Table 10-9.

- The unsupported length of the test beam was based on the length of the W27x84 beam.

- The distance from the load to the beam end was specified to induce similar rotation to a uniformly loaded beam. (App. B)

- The point load to cause the reaction is the load at which the end reaction is reached.

For the analysis of the loading strategy, see Appendix B.

For the calculations that show that the W27x84 was free of residual stresses in all tests, see Appendix C.

For a sample deflection and rotation calculation see Appendix D.

For a sample shear tab design using Table 10-9 of the Manual see Appendix E.

Description of the Test Setup

The test was performed using a cambering machine at a steel fabrication shop, Wylie Steel, Inc., in Springfield, Tennessee. The column and opposite end of the beam were laid flat (horizontally) on the bed of the cambering machine and were supported by the wall of the cambering machine. A support was welded onto the machine so the hydraulic loading jack could load the beam perpendicular to the supporting wall. See Figures 5 and 6 below for diagrams of the testing setup.
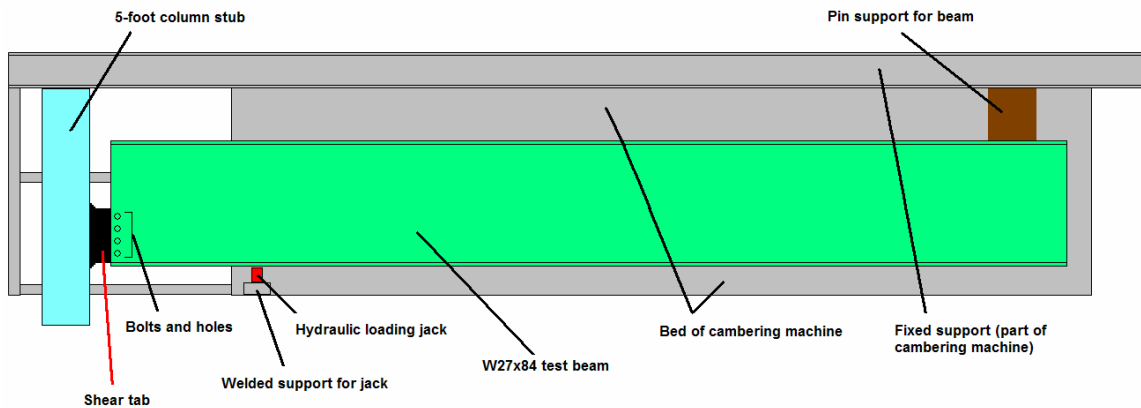
Figure 9: Plan view of the test setup
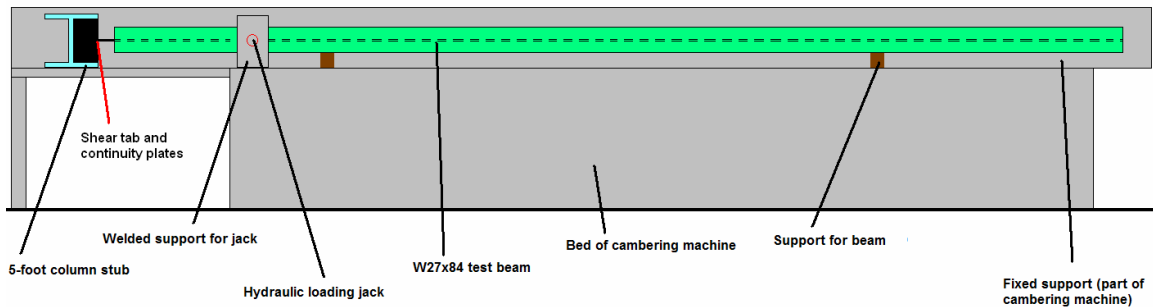
Figure 10: Elevation view of the test setup

The column stub, shear tab, and beam were all provided and fabricated by Wylie Steel, and all preparation work done on the cambering machine was done with assistance from Wylie Steel. The 100-ton loading jack was provided by Geosciences Design Group of Nashville, Tennessee, and it was calibrated the day before the first session of testing, so the loading information was very precise.

16

Test Session 1

The connection details for the first test session were based on a design load of 44.7 kips. The connection was designed based on Table 10-9 of the AISC Manual, page 10-119, and it was determined that four bolts were needed with a 3/8" shear tab and 5/16" fillet welds.

For validating the results of the finite element modeling, the strain values at selected locations for different load levels were needed. These strain values could then be converted to stress values using appropriate constitutive relationships up to the limit state. The standard method for measuring strains in such a test is strain gage instrumentation. Since strain gages were not available at the time of session 1, an attempt was made to use a mechanical extensometer, or Demec gage, to measure the strains. The extensometer measurements, however, were found to be unreliable because of problems with the studs used to mark the gage points. As a result, the strain data from session 1 was ignored and the only relevant data was the load at each interval, the beam's corresponding maximum deflection, and the buckling load. In addition, video highlights of the test were recorded so the effects of the beam, column and shear tab could be seen. It was evident in session 1 that the load capacity of the extended shear tab greatly exceeded the design load.

In comparing the two tests of session 1, the deflection data at each interval was exactly the same, but the connection in Test 1-1 held more load. Therefore, the final deflection was different for the two tests. However, in both tests the connection showed no noticeable deformations until a reaction of 90 kips was reached.

Buckling of the Test 1-1 shear tab was first noticed when the reaction reached around 90 kips. As the load was further increased, the plate buckling continued until it would hold no more load. The buckling occurred at the bottom of the effective, or extended, region of the plate.

When the reaction reached approximately 90 kips in the second test of the session, buckling was observed in the same region of the plate as in the first test. After the load was increased further, it was determined that the connection was unstable and testing was halted.

After disassembly, some interesting observations were noted. In the first test, the holes were moderately deformed from their original short-slotted (SSL) shape and the shear tab had buckled

significantly. The shear tab remained in the buckled position long after the load was removed, indicating some plastic deformation. Also, the bolts were slightly damaged, but they were far from failure.

In the second test, the holes were slightly less deformed and the shear tab buckled about the same extent as in the first test. Again, the buckling deformation in the shear tab was not recovered after the load was removed, signaling plastic deformation. Also, the condition of the bolts in the second test was similar to the first test, that is, slightly damaged but far from failure.

One dilemma of session 1 was the fact that the column was found to rotate a good amount, since it was not fixed at its base. In order to correct this problem in the following tests, a base plate was welded to the base of the column and subsequently fixed to the support.

The following photographs (Figures 11-19) show the EST connection at different stages of testing during session 1. Figures 11 and 12 show the connection before the beam was bolted to it. Figures 13 and 14 show the connection after the beam has been bolted to the EST and gage studs have been glued for measuring strain using the extensometer. Figure 15 is a closeup view of the extensometer used to take the strain readings. In Figure 16 the hand-operated jack lever used to apply the load is shown along with the gage. Figure 17 shows the lever being cranked to apply the load through the hydraulic cylinder. Figure 18 shows the strain measurement technique with the extensometer. Figure 19 is a snapshot taken after the buckling had occurred and the plate is in its deformed shape. Rotation of the column, which was not fixed at its base, is evident in Figure 20. The permanent deformation of the shear tab can be seen in Figures 21 and 22, which were taken after the connections were disassembled.   The deformation of the shear tab at the bolt holes is apparent from Figure 23, confirming that the connection behaved as bearing type at its limit state.
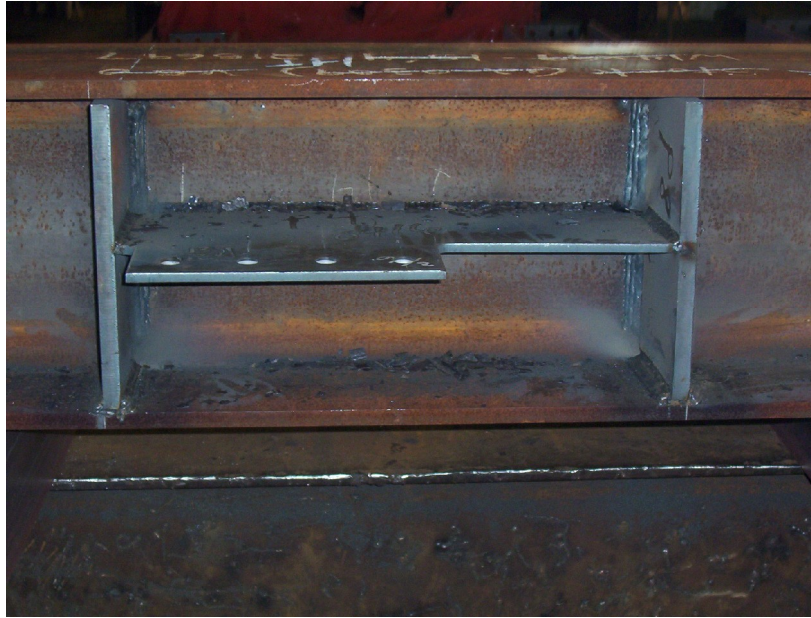
Figure 11: Connection before testing was performed

Figure 12: A closeup of the shear tab before testing

Figure 13: The connection, beam end and column stub before testing

Figure 14: A closeup of the connection before testing

Figure 15: A closeup of the extensometer used to measure strain
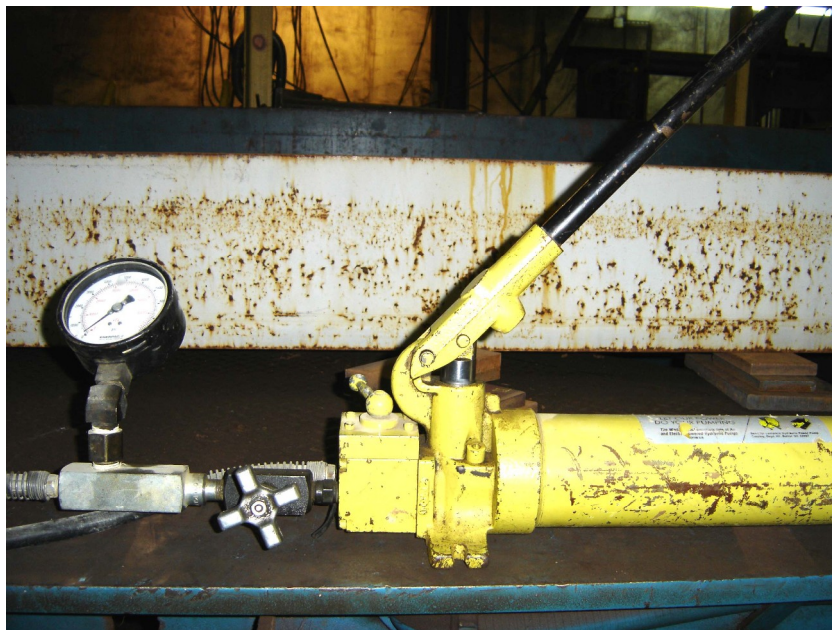
Figure 16: The lever and gauge of the hydraulic loading jack

Figure 17: Load application using the hydraulic jack

Figure 18: Using the extensometer to measure strain during testing
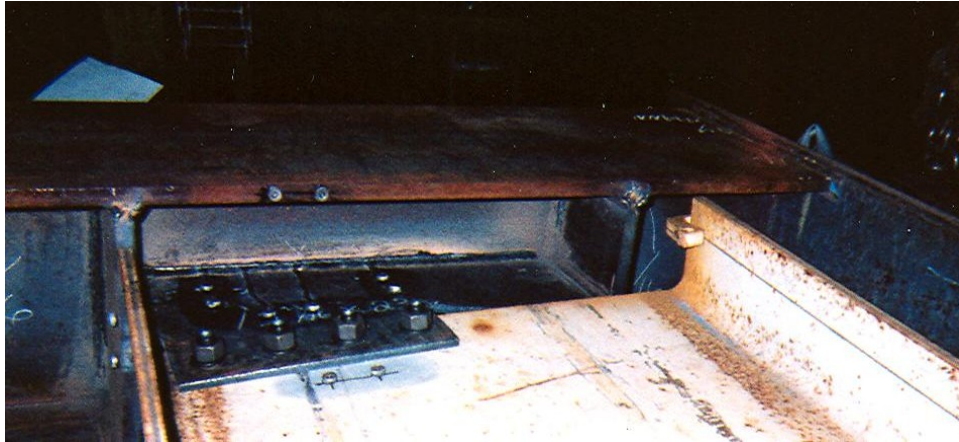
Figure 19: The buckled shear tab after testing

Figure 20: Rotation of the beam at the end of testing (space from flanges to column)

Figure 21: The buckled shear tab of test 1-1
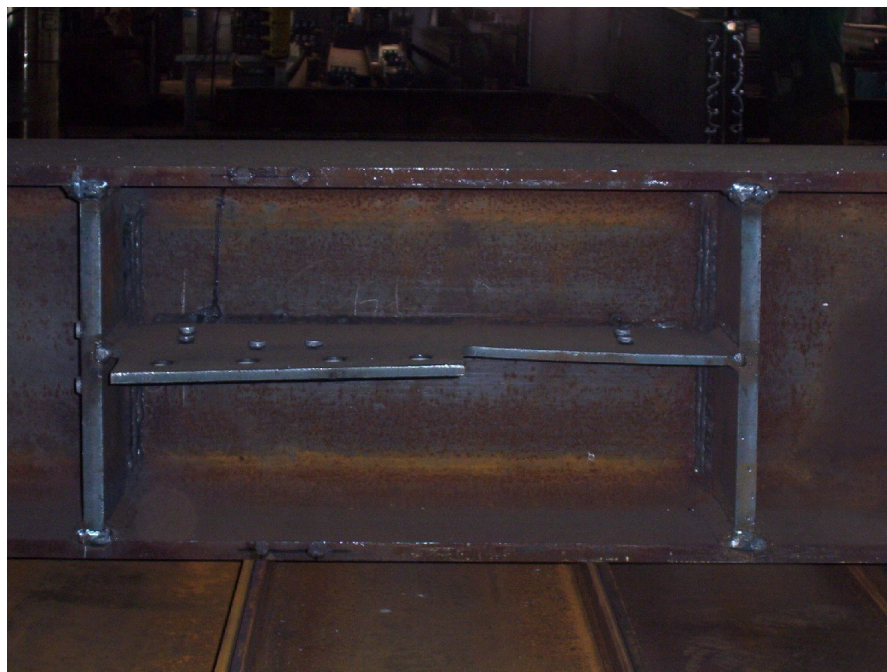
Figure 22: The buckled shear tab of test 1-2

Figure 23: The shear tab holes of test 1-1 after testing

Test Session 2

For the second test session the connection details were based on a load of 27.8 kips. Using Table 10-9 of the AISC Manual, page 10-120, it was determined that four bolts were needed with a ¼" shear tab and 3/16" fillet welds.

Strain Gages

In this session, due to the unacceptable strain data in session 1, the mechanical strain gage was replaced by electrical strain gages. Six strain gages were used for each test in session 2, located on the following:

1. The top of the top flange of the beam at the centerline, measuring the compression due to bending of the beam,

2. The beam situated vertically near the bolts, measuring the vertical stresses in the beam web,

3. The top of the top continuity plate at the centerline, measuring the compression due to bending of the plate,

4. The shear tab situated horizontally at the top, to measure the tension due to the moment developed in the tab,

5. The shear tab situated horizontally at the cope, to measure the compression due to the moment developed in the tab, and

6. The shear tab situated vertically near the bolts, to measure the vertical stresses in the tab.

The following Figures are some photos of the strain gages and strain gage equipment. The strain gages were from Omega and were model number KFG-5-120-C1-11L1M2R. Their nominal resistance was 120 ohms and they were encapsulated with two attached lead wires. The equipment used to get the output from the strain gages was a Vishay / Ellis – 20 digital strain indicator with a Vishay / Ellis – 21 channel selector. Figure 24 shows the Vishay / Ellis equipment and some of the connected strain gages. Figure 25 shows in detail the location of strain gages 2, 4, 5, and 6.

Figure 24: Equipment used to obtain readings from strain gages

Figure 25: Strain gages at locations 2, 4, 5, and 6

The strain indicator was calibrated before the testing and with its output, strains could be found at different loads. Subsequently using Hooke's Law, the stresses at those locations and load levels could also be calculated. The following is a qualitative review of the strain gage and stress results.

- The sign of the strains was consistent with expectations; in other words, where compression was expected, compression was measured, and where tension was expected, tension was measured.

- The critical stresses were from locations 4, 5, and 6 on the shear tab, shown in Figure 26. These corresponded to the failure mode of buckling in the tab that was witnessed in both tests.

- Some strains far exceeded the nominal ultimate strain of the plate, equivalent to a stress of 58 ksi. This is to be expected due to the plastic flow of steel past its yield point.

- The stresses at the top of the beam flange at the centerline of the beam were compressive and linear, indicating that the beam was receiving the load and remained elastic. Also, after unloading the beam, the strain gage reading returned to zero, meaning that the there were no residual strains nor stresses.

- After unloading the beam, some of the strains had some residual strains. This confirmed the occurrence of plastic deformation, which was visually evident from the permanent deformation in the shear tab.
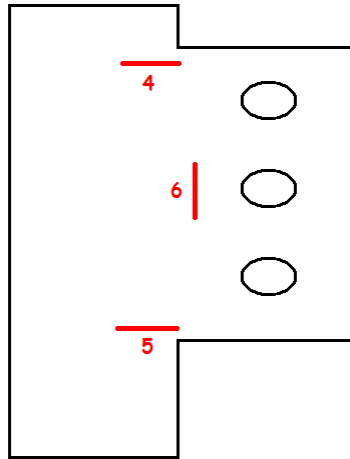
Figure 26: Crucial strain gages at locations 4, 5, and 6

- One interesting observation from the stress and strain data was the behavior of strains measured at locations 5 and 6 near the limit state. Again, the strain gage at location 5 was placed horizontally at the bottom of the effective region of the tab, along the buckling line. The strain gage at location 6 was oriented vertically on the tab near the bolts, essentially the compressed part that buckles. Though the readings at location 6 jumped dramatically as buckling occurred, when the load was removed, the readings dropped somewhat. The readings at location 5 didn't jump too high during the buckling process, but when the load was removed, the strain reading changed dramatically. This may be attributed to the condition that location 5 behaved elastically throughout while location 6 underwent plastic deformation. Upon load removal, a redistribution of the stresses occurred, which led to the noted behavior.

<u>Tab Deformation</u>

Both plates carried approximately the same load before buckling. Buckling was first noticed at a reaction of around 63 kips. The connection held a little more load and then failed at 66 kips. In both cases,

the buckling deformation of the tabs was not recovered upon removal of the load. Also, the buckled shape and location in the two tests resembled each other closely. See Figure 27 for the buckled shape of one of the shear tabs.
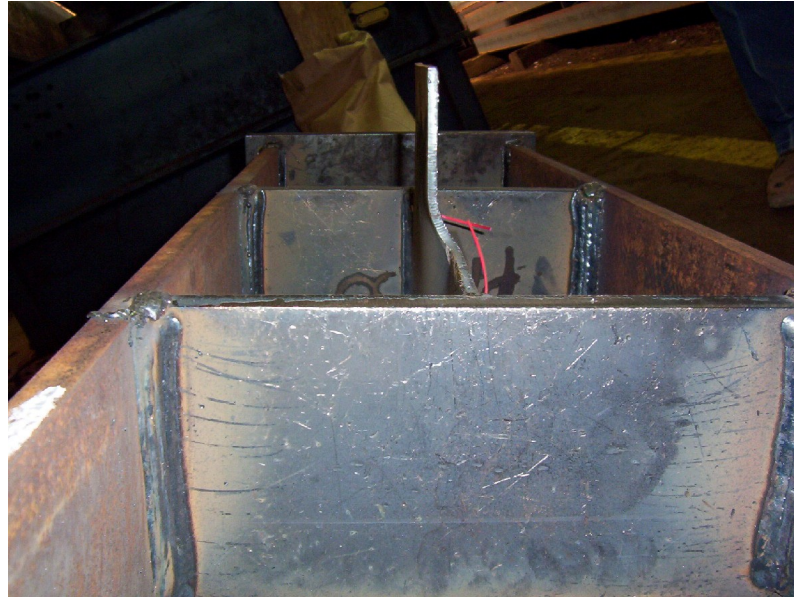
Figure 27: Buckled shape of the shear tab after unloading and disconnecting

Hole Deformation

In both tests, the bolts were snug-tight, bearing-type. At the limit state, the holes experienced considerable damage due to the bolts bearing on them. The damage appeared as an indentation at the bottom of the holes, in the direction of the load. The damage to the holes for both tests looked very similar after disassembly, as shown in Figure 28.

Figure 28: Deformed short-slotted holes after the test and disassembly

Bolt Deformation

In this session, the bolts used in the connection were not damaged enough to be noticed by the naked eye. There was almost no noticeable damage to the threads of the bolts.

Column Base Fixity

In session 1, one of the problems with the test was that the column rotated significantly about its base and in the process failed to satisfy the real-world conditions. To correct this problem in session 2, a base plate was welded to the base of the column and some shim plates were used to make the column square to the beam, as shown in Figure 29. These shim plates were needed to offset the imperfections of the cambering machine's support. The base plates were then tied to the cambering machine's support by using heavy-duty C-clamps. The consensus was that in both tests this method worked, as very little or no rotation was noticed at the column base and top.
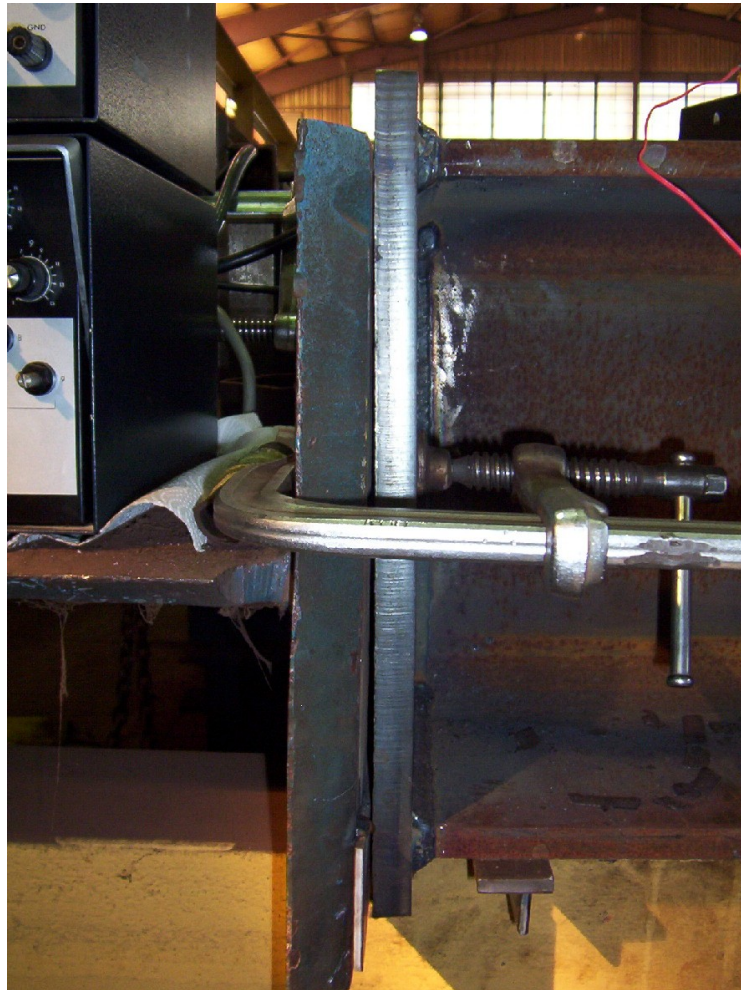
Figure 29: C-clamp and base plate used to fix the column base to the support

Test Session 3

In the third session, the design load was 27.8 kips. However, because the failure mode in the first two sessions was the same, an attempt was made to force the failure mode away from the plate and onto the welds or the bolts. Thus, the plate thickness was designed very conservatively in session 3. The connection was designed based on Table 10-9 of the AISC Manual, page 10-120, and it was determined that four bolts were needed with a ¼" shear tab and 5/16" fillet welds. In an attempt to force the failure mode away from the shear tab, a plate thickness of ½" was used in these two tests.

<u>Strain Gages</u>

Similar to session 2, strain gages were used in session 3. Seven strain gages were used for the tests in this session, at the following locations:

1. The top of the top flange of the beam at the centerline, measuring the compression due to bending of the beam

2. The beam situated vertically near the bolts, measuring the vertical stresses in the beam web

3. The top of the top continuity plate at the centerline, measuring the compression due to bending of the plate

4. The top of the top continuity plate at the centerline, measuring the tension due to the moment developed in the tab

5. The shear tab situated horizontally at the top, to measure the tension due to the moment developed in the tab

6. The shear tab situated horizontally at the cope, to measure the compression due to the moment developed in the tab

7. The shear tab situated vertically near the bolts, to measure the vertical stresses in the tab

Figure 30 shows strain gage 4 on the right, the only new gage in this test. Also in the Figure is strain gage 3. The strain gages and output equipment used were the same as in session 2.
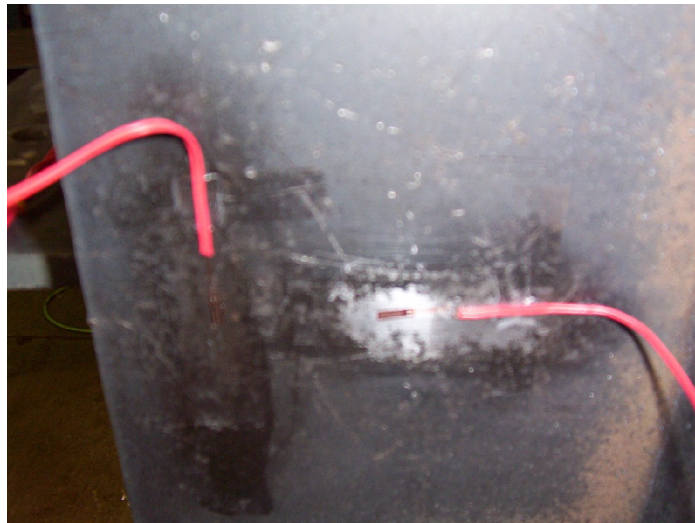
Figure 30: Strain gage 4, shown on the right, was the only new strain gage for this session

The strain indicator was again calibrated before the session and the strain output was to be converted to stresses using Hooke's Law again. The following is a qualitative review of the strain gage and stress results. Much of this review is similar to the session 2 review.

- The sign of the strains was consistent with expectations; in other words, where compression was expected, compression was measured and where tension was expected, tension was measured.

- The critical stresses were from locations 5, 6, and 7 on the shear tab, and these corresponded to the failure mode of buckling in the tab that was witnessed in both tests.

- Some strains far exceeded the nominal ultimate strain of the plate, equivalent to a stress of 58 ksi. This is to be expected due to the plastic flow of steel past its yield point.

- The stresses at the top of the beam flange at the centerline of the beam were compressive and linear, indicating that the beam was receiving the load and remained elastic. Also, after unloading the beam, its measurement returned to approximately zero.

- After unloading the beam, some of the strain gages had some residual strains. This confirmed the occurrence of plastic deformation, which was evident from the permanent deformation of the shear tab.

- One interesting observation from the stress and strain data was the behavior of strains measured at locations 6 and 7 at the limit state and after unloading compared to those of session 2. Again, the strain gage at location 6 was situated horizontally at the bottom of the effective region of the tab, along the buckling line. The strain gage placed at location 7 was oriented vertically on the tab near the bolts, essentially under compression and prone to buckling. In this session, the strain readings of both the gages jumped dramatically during the buckling process and both dropped somewhat after the load was removed. The behavior of the two strain gages agreed more than those of session 2, when the strain readings went in opposite directions.

Tab Deformation

Both tests carried approximately the same load before buckling. Buckling was first noticed around a reaction of 95 kips. The connection held some additional load and finally failed at 102 kips. For

both plates the buckled shape was not recovered and showed close resemblance. Figure 31 shows the buckled shape of one of the shear tabs after unloading and disassembly.
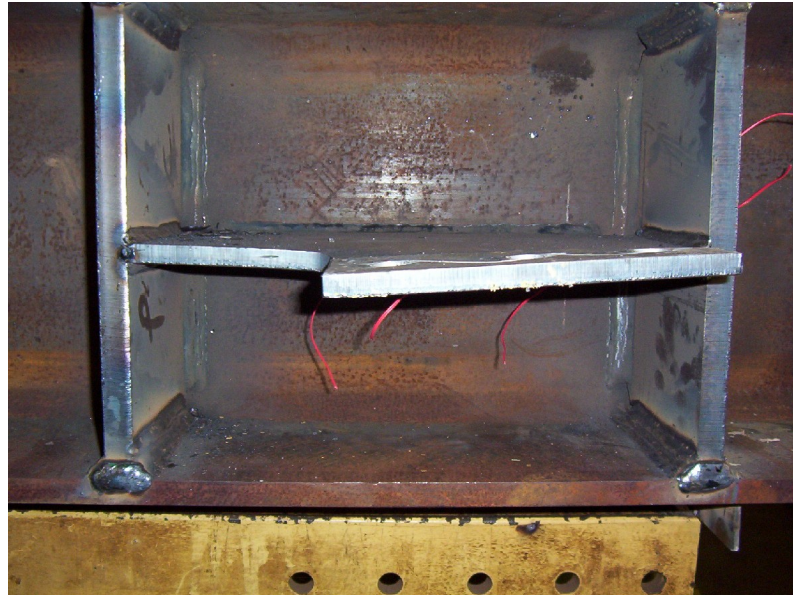
Figure 31: The buckled shape of one of the shear tabs from session 3 after unloading and disassembly

Hole Deformation

In this session, both tests were run using snug-tight, bearing-type holes. The holes experienced significantly less damage due to the increased thickness of the plate. Again, the damage appeared as an indentation on the bottom of the holes, in the direction of the load. The damaged holes for both the tests looked very similar after disassembly, as shown in Figure 32.

Figure 32: The deformed shape of the SSL holes from session 3 after the test was completed

Bolt Deformation

      In this session, the bolts were damaged more than in the other two sessions, simply because the load experienced by each bolt was the highest in this session. There was noticeable damage to the thread, as evident from Figure 33.

Column Base Fixity

      As in session 2, a base plate was welded to the base of the column and some shim plates were used to make the column square to the beam. These shim plates were needed to offset the imperfections in the cambering machine's support system. The base plates were then tied to the cambering machine's support using heavy-duty C-clamps.

Figure 33: The deformation of the middle bolt from session 3 after the bolts were disconnected

<u>Uplift of Beam and Column</u>

One new problem arose during the two tests in this session. When the shear tab started to buckle, it caused the beam and the column to lift up and off the support bed, as shown in Figure 34. This may be attributed to the fact that the beam and column were not pinned down during the test. In previous tests, the self-weight of these members was adequate to prevent lifting off the support bed. However, in the session 3 tests, the shear tab being sufficiently strong, as the load was increased, the limit state was reached by causing lateral-torsional buckling of the beam. It is believed that the connection could have supported more load if the column and beam were laterally restrained against lifting off the test bed. This lift-off phenomenon is shown in Figures 34-36.

Figure 34: The column lifting off its support due to lateral-torsional buckling of the beam

Figure 35: The beam lifting off its support due to lateral-torsional buckling
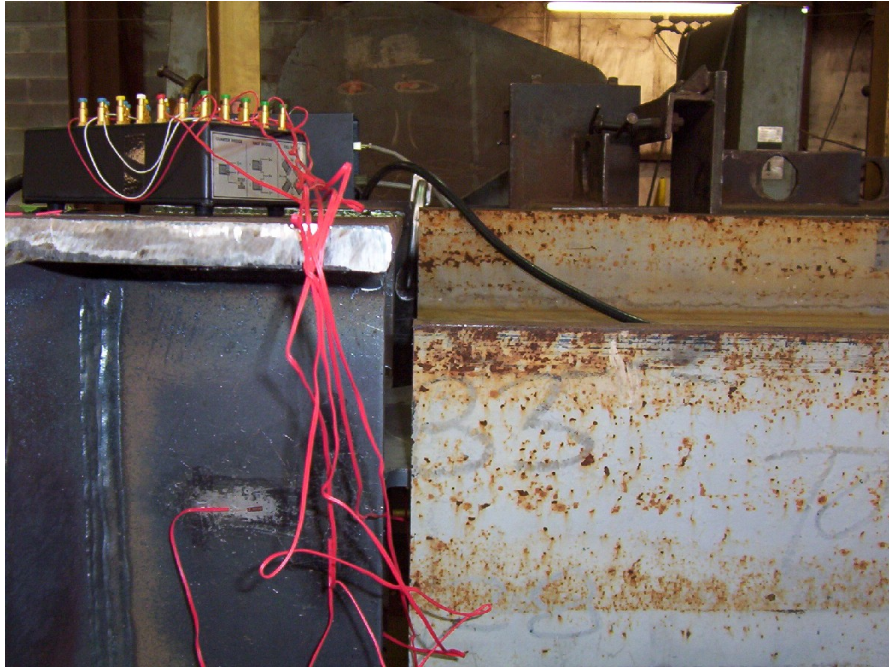
Figure 36: The rotation of the beam relative to the column due to lateral-torsional buckling of the beam (the far flange of the beam is much higher relative to the column than the near flange of the beam)

CHAPTER V

FINITE ELEMENT MODELING

Overview of the Modeling Program

For computer simulation of the extended shear tab connections considered, finite element modeling was used. Such simulation will not only help validate the test data and vice-versa, it will also enable studying many more cases without the need for undertaking expensive and time-consuming experimental investigation. For the purpose of the present study, computer modeling was undertaken using the commercial software ANSYS (Version 7.0), accessible through the High-Performance Computer Laboratories (HPCL) at Vanderbilt University. The lab computers were SUN Microsystems running a UNIX operating system.

In all, many cases were considered, but only four cases are reported herein. After attempting to run models with different degrees of complexity, it was concluded that the ones reported yielded the most consistent and accurate results. Each model was three-dimensional and consisted of an extended shear tab and two continuity plates. The shear tab was made continuous ("glued") to both continuity plates. The continuity plates had fixed boundary conditions along all welded edges, as did the one edge of the shear tab. All modeling was done at full scale, so the sizes of the plates and members in the models exactly represented the fabricated sizes of the plates. Loading consisted of pressures only because forces applied on discrete points would have led to excessive localization of the stresses around these points. See Figure 37 for a closeup view of the pressure loading. Of the four models, two simulated the shear tabs in testing session 2 (models 2-A and 2-B) and two simulated the shear tabs in testing session 3 (models 3-A and 3-B). All models used pressure applied directly on the lower flat part of the shear tab holes only.

As mentioned earlier, the modeling procedure described above was not the only procedure that was undertaken. Many other simulations were run, but the results of other simulations did not match the accuracy or consistency of the results of the above model. Some of the other models that were tried are listed next, along with the reason for not making the final list.
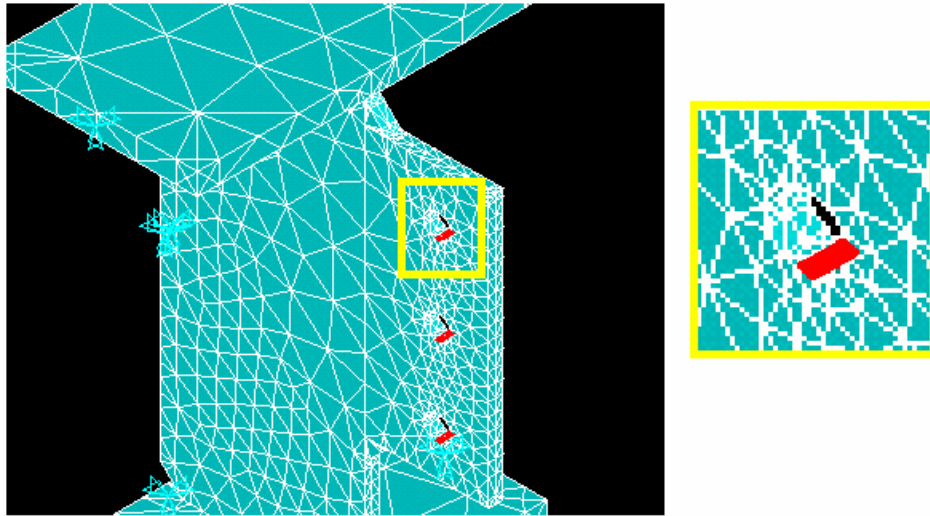
Figure 37: A closeup view of the pressure load used in the finite element models

- Models with the column and beam included were run but were not reported due to the members' minimal effect on the model results.
- Two-dimensional models were run with triangular six-node elements but they also yielded worse results because the continuity plates could not be modeled properly.
- An attempt was made to apply the pressure on a cylindrical bolt and to use contact elements through the contact wizard feature of ANSYS to model the interaction between the bolt and the shear tab. However, reliable results could not be obtained with this model refinement and, therefore, those models were not reported.

The pressure loading in the models needed to be determined to represent one of the reactions from the testing sessions. Since the holes in each model were short-slotted, the pressure was applied on the flat surface of the short slotted hole that is 3/16" x the thickness of the shear tab. It was assumed that the applied load was equally shared by the holes

The loading details of the four cases are shown in Table 2. The only difference between session 2 and session 3 models was in the thickness of the shear tab. The "A" models were run with a load that was small enough to keep the models elastic. Mechanical properties of steel from Wylie Steel were used based on the mill reports of the steel used in the tests. According to the mill reports, the yield strength of the plates was 46.6 ksi and the ultimate strength was 69.8 ksi. In the "A" models, the only material property

input was Young's Modulus (29,000 ksi) and Poisson's ratio (0.31). The "B" models were run with a

higher load, specifically, the load at which buckling was initially encountered. Because an attempt was

made to model plastic deformation, the properties of the steel were crucial in the analysis. Since it was

necessary to identify the state of the connection at the limit point, it was decided that the properties

corresponding to that state were essential. This was done by representing the state based on the ultimate

tensile strength of the material and the corresponding strain, leading to a secant modulus value of

E = / = 70 ksi / .14 = 500 ksi. E for the "B" models was 500 ksi and Poisson's ratio remained 0.31.

Table 2: Loading information for each of the finite element models

MODEL	MODEL 2A	MODEL 2B	MODEL 3A	MODEL 3B
Thickness of Shear Tab	¼"	¼"	½"	½"
Area of Pressure	.046875	.046875	.09375	.09375
Reaction	30 kips	66 kips	30 kips	90 kips
Each Hole Reaction	10 kips	22 kips	10 kips	30 kips
Pressure Value Used	213.3	469.3	106.7	320

In general, the procedure used to create and run each of the models is listed below. For a more

detailed procedure, see Appendix F.

- The model type was chosen as Structural.

- The element type was chosen (Tetrahedral 10-node 187 in the ANSYS element library).

- The material properties were input.

- The three-dimensional geometry was created and meshed.

- The boundary conditions and pressures were applied.

- The model was solved.

- The desired output was plotted and listed

Output of Model 2-B

The real computational time for most models was ten seconds, never exceeding one minute. The

typical number of elements was around 10,000. The screenshots shown in Figures 38-46 illustrate some of

the plotted and listed input and output for Model 2-B. The results of the other three models were similar to the following screenshots.
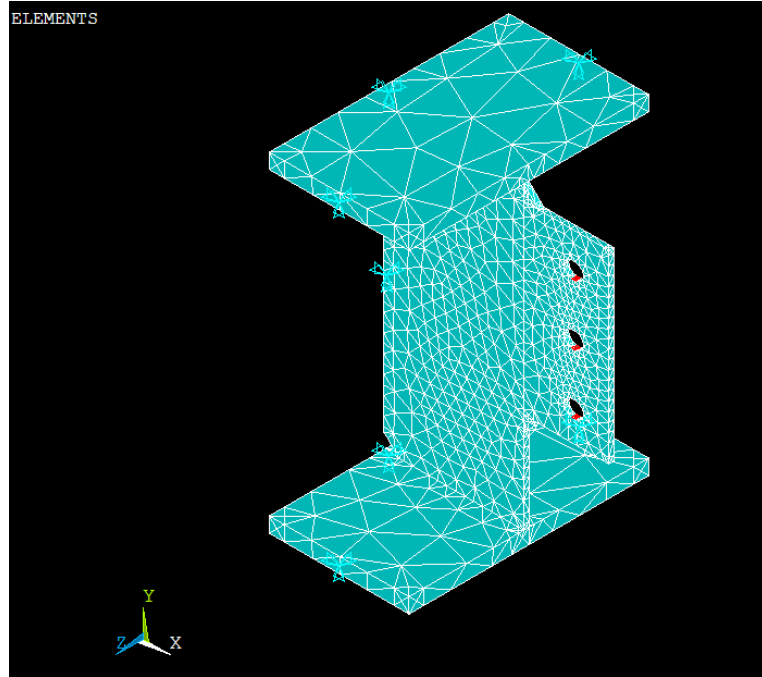
Figure 38: The mesh, boundary conditions, and pressures of Model 2-B
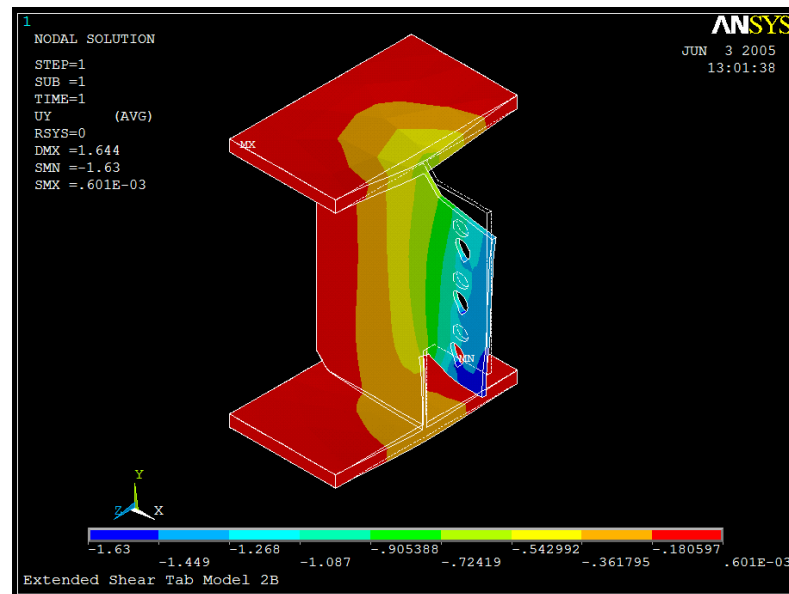
Figure 39: The Global Y-displacement due to the buckling load of Model 2-B
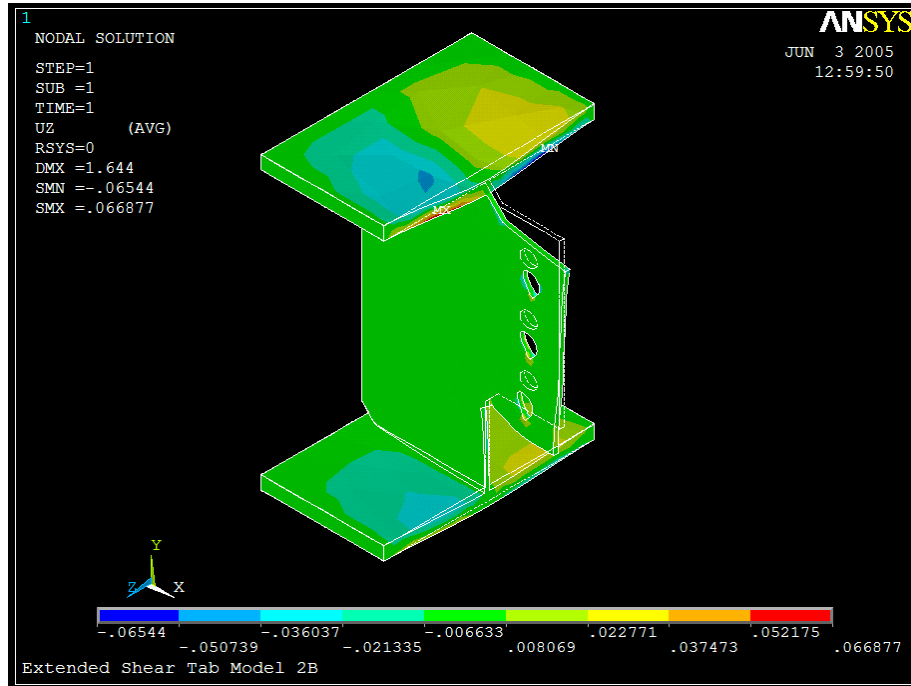
Figure 40: The Global Z-displacement due to the buckling load of Model 2-B
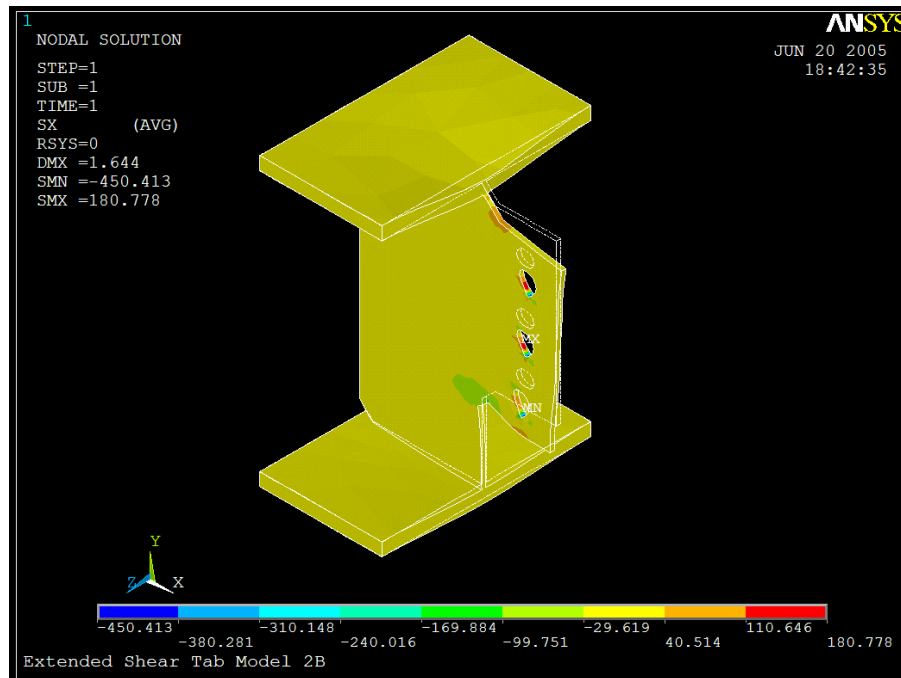
Figure 41: The stress component in the Global X-direction of Model 2-B

Figure 42: The stress component in the Global Y-direction of Model 2-B
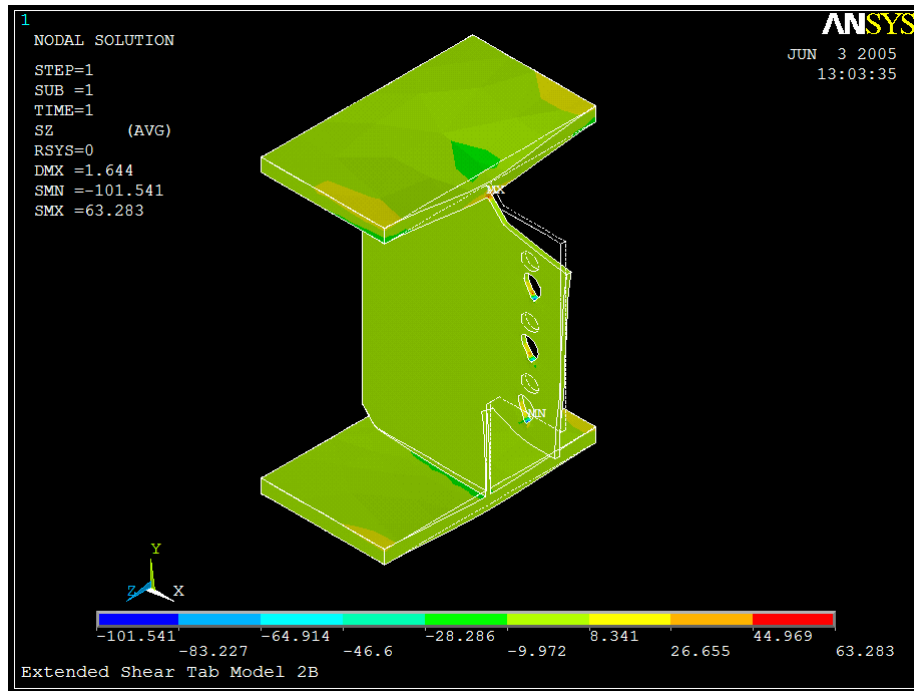
Figure 43: The stress component in the Global Z-direction of Model 2-B
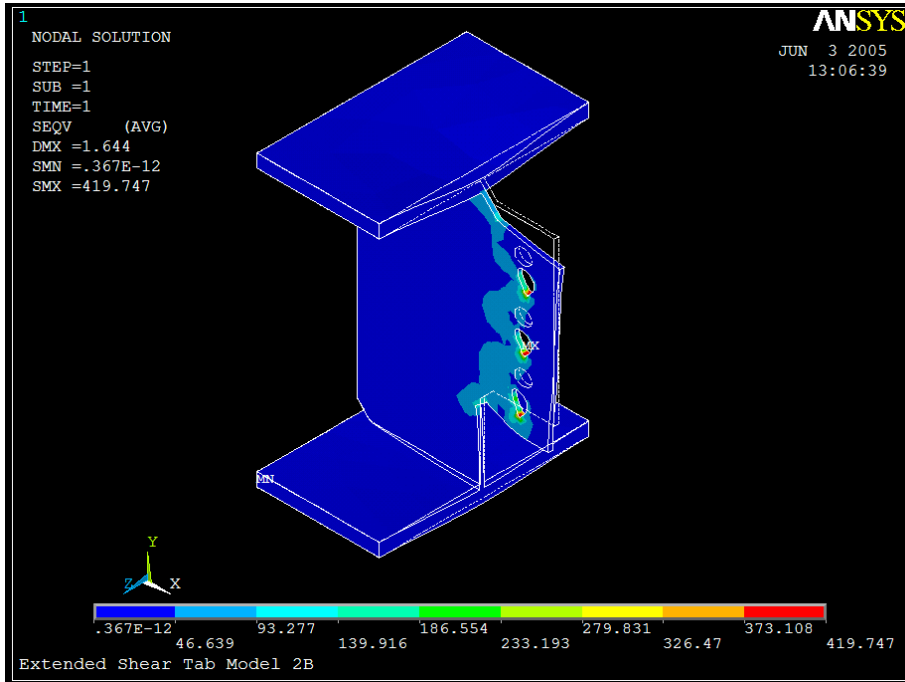
Figure 44: The von Mises equivalent stress values for the buckling load of Model 2-B

```
                         PRINT S    NODAL SOLUTION PER NODE


                       ***** POST1 NODAL STRESS LISTING *****

                         PowerGraphics Is Currently Enabled


                         LOAD STEP=     1  SUBSTEP=      1

                         TIME=    1.0000      LOAD CASE=   0

                         NODAL RESULTS ARE FOR MATERIAL    1


                  THE FOLLOWING X,Y,Z VALUES ARE IN GLOBAL COORDINATES


       NODE    SX           SY           SZ           SXY          SYZ          SXZ
         1   15.477       108.95        6.0322        5.0240       0.36361      0.11733

         2  -12.204      -0.47270     -0.25524       -1.7394      -0.21974      0.19840

         3  -10.308      -44.687      -13.533       -15.648        3.5737       2.6981

         4 -0.29346       5.7600       -7.8068       -0.93481     -0.33270      1.2123

         5   0.19105      7.0505       -8.2760       -1.3428       0.89164     -1.0818

         6  -61.192      -135.32       -8.5757       -70.810      -4.1331      -1.3440

         7  0.60134E-01-0.30627      -0.42939E-01-0.44384       -0.12811      -0.19472

         8  -150.62      -68.373       -8.5001       -80.115       2.5826       3.5803

         9  -62.327      -143.46       -6.7182       -75.026       3.3130       1.5791

        10   0.17294      0.16734     -0.86841E-01-0.20931       -0.66369E-01-0.22276E-01

        11  -43.466      -42.166      -0.61412E-01 -28.755        0.50666E-01 0.13461

        12   35.873       23.714       0.12309E-01 -24.896        0.18961E-01-0.19735E-01

        13  -43.468      -42.070      -0.23450E-01 -28.615        0.11915      -0.53487E-01

        14  -213.30      -209.83      -13.520        145.96       -5.7888       11.653
```

Figure 45: Listing of stress components by node number for Model 2-B

46

Output of Other Models

The following Figures, on a smaller scale, show the output plots of Models 2-A, 3-A and 3-B.
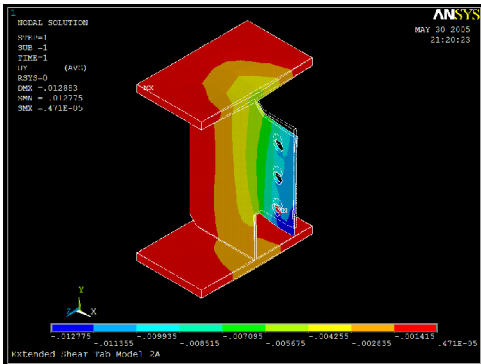
Figure 46: Y-displacement plot of Model 2-A
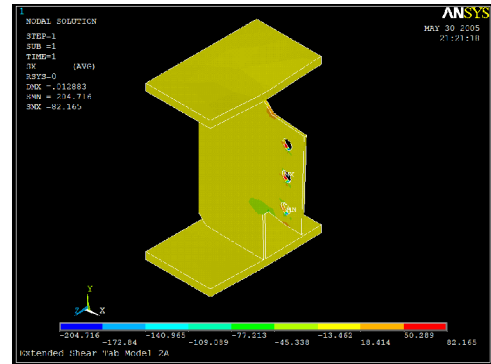
Figure 47: X-Stress plot of Model 2-A

Figure 48: Y-Stress plot of Model 2-A
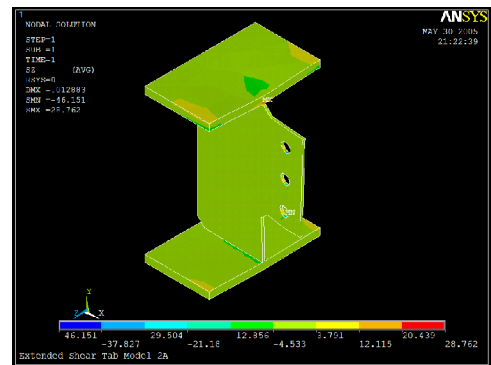
Figure 49: Z-Stress plot of Model 2-A
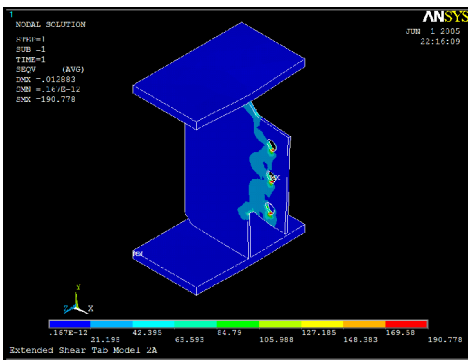
Figure 50: Von Mises Stress plot of Model 2-A
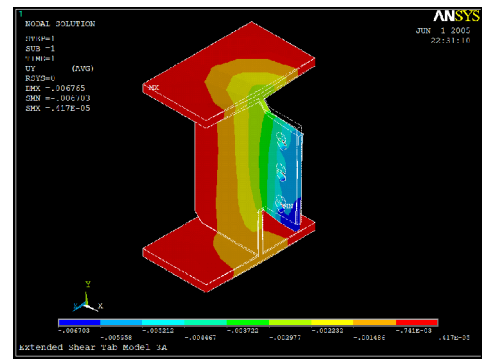
Figure 51: Y-Displacement plot of Model 3-A
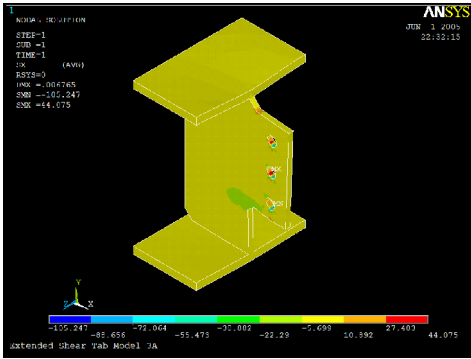
Figure 52: X-Stress plot of Model 3-A
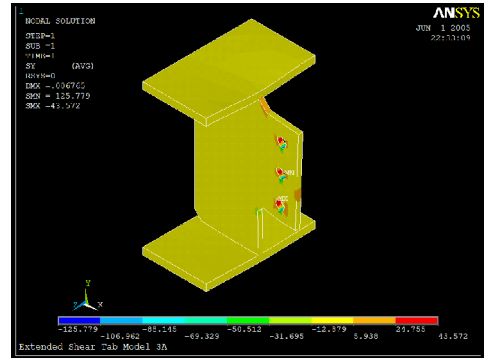
Figure 53: Y-Stress plot of Model 3-A
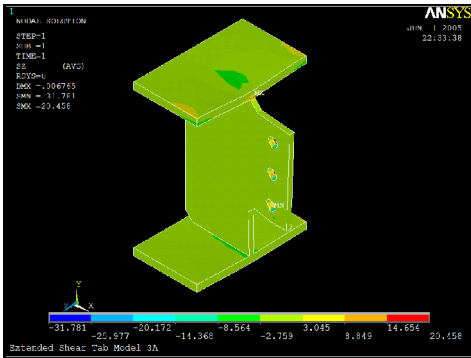
Figure 54: Z-Stress plot of Model 3-A
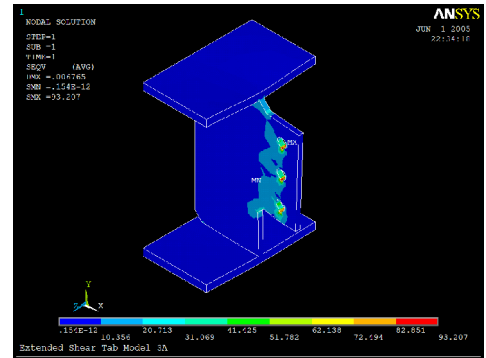
Figure 55: Von Mises Stress plot of Model 3-A
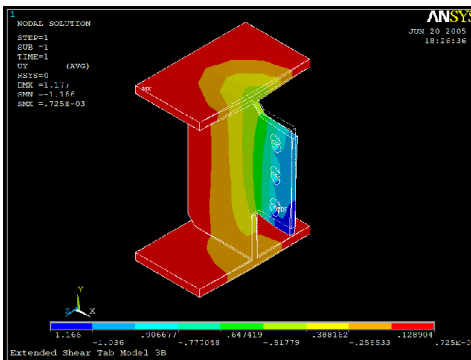
Figure 56: Y-Displacement plot of Model 3-B
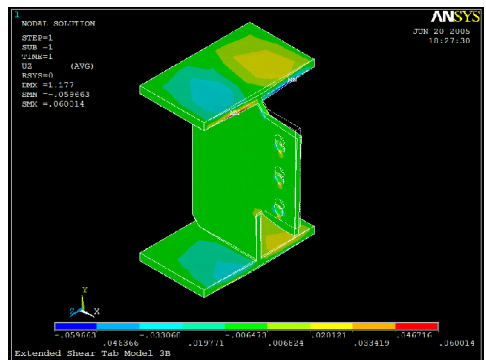
Figure 57: Z-Displacement plot of Model 3-B
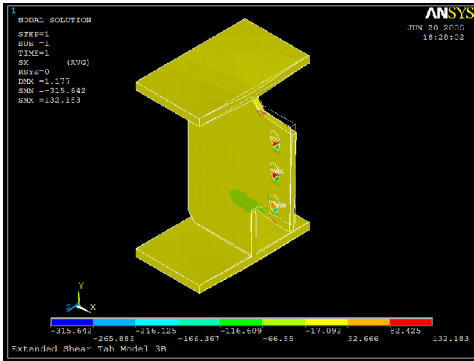
Figure 58: X-Stress plot of Model 3-B
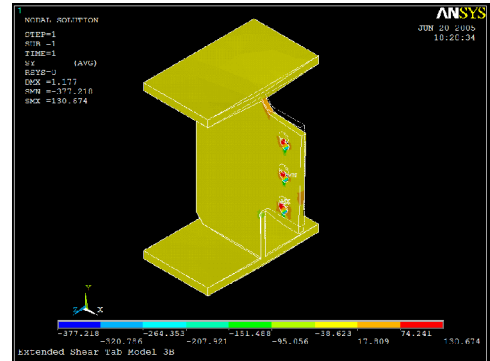
Figure 59: Y-Stress plot of Model 3-B
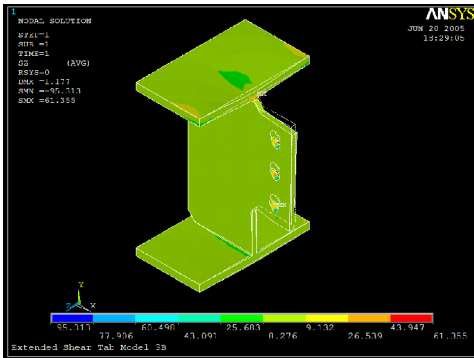
Figure 60: Z-Stress plot of Model 3-B
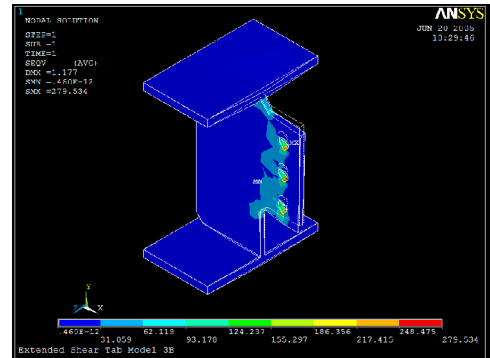
Figure 61: Von Mises Stress plot of Model 3-B

It can be seen from the above plots that the stresses and displacements near the holes were much higher than those a greater distance away from the holes. This is expected, due to the concentration of stresses around irregularities in the geometry, but the severity of the concentrations in the above models is believed to be a little too high.

CHAPTER VI

RESULTS, COMPARISONS, AND CONCLUSIONS

Summary of Test Data

The following table lists some general results from each session of the testing phase so that the

sessions can be compared to one another.

Table 3: Summary of test results

Result	Session 1	Session 2	Session 3
Factor of Safety = Ultimate load capacity / Design load	2.3	2.4	3.7
Were the beam deflections and strains on target?	Yes	Yes	Yes
Was plate buckling the failure mode?	Yes	Yes	Yes
Had the plate compressive strains exceeded F_y at failure?	Yes	Yes	Yes
Hole Damage Rating (1 – minimal ; 10 – failure)	5	6	3
Bolt Damage Rating (1 – minimal ; 10 – failure)	3	1	8

Overall the testing phase showed that the extended shear tabs could support over twice the load for

which they were designed. All the strains and deflections indicated that the load was being transferred

properly from the hydraulic jack to the beam and finally to the connection. The testing data and results

support the hypothesis. The smallest safety factor was 2.3 and the largest was 3.7, which well exceed, by

comparison, the allowable stress design safety factor of 1.67. In all cases, the limit state was characterized

by buckling and yielding of the shear tab.

Summary of Modeling Data

In general, the procedure used to model the extended shear tabs in this project is very approximate.

Many assumptions and estimations were made and a more exact method could definitely be used.

However, due to time limitations, the procedure used can be considered a good first step. An analysis of

the finite element model results shows that at the nodes around the holes, the stresses in all directions were

very large, but a short distance away from the holes the stresses became much smaller. This is expected in an inelastic analysis that is run with elastic material behavior. At the higher loads, the stresses at high stress gradient points (near holes and load points) are bound to be unrealistically high, well exceeding the yield strength. Moreover, the load application was not representative of the true pressure distribution created by the connection bolts. Another problem with the models was that the boundary conditions allowed almost no rotation of the plates, causing deflections and strains to be considerably lower than the observed values. Simulating the welded connections of the shear tab and continuity plates to the column as fixed boundary conditions may have created a system that was too rigid. A possible resolution to this problem would be to model a full-scale column and fix its ends, and then the plates could be glued to the column. However, several test models were run, each with over 10,000 times the number of elements of the reported models, using a 15-foot column and a full-scale 25-foot beam, but the results were no better. Therefore, it was concluded that the beam and column were not essential components of the models.

The above analysis demonstrated the need for using more refined models in the sense that the material behavior should be characterized accurately and that geometric nonlinearity should be included so that the buckling phenomenon at the limit load could be truthfully reproduced. This refinement does not however call for including the beam and column in the model. In spite of the stated shortcomings, the models did produce some positive results. The signs and magnitudes of stresses, especially away from the holes, were near expected values.

Modeling Data vs. Test Data

In the testing phase, the strains were measured at different locations under different loads. The strain gages were uniaxial, so the strains were measured in one direction only. The strains were then converted to stresses using Hooke's Law. In the modeling phase, two of the marked loads from the testing phase were chosen as the model loads so that the stresses could be compared to the testing stresses. The stress-listing output of the models was for six stress components. To compare the modeling data to the test data, the stress components extracted from the model output were chosen to match the direction of the strain gage from the tests. Table 4 lists the stresses at the different load levels and locations for the models

and the tests. The discrepancy between the test and model results can be attributed to the antiquated data acquisition system used in the tests or modeling error.

Table 4: Modeling data vs. test data at different load levels and locations

Analytical vs. Experimental Stresses for 1/4" Shear Tab (Session and Models 2)				
	STRESSES (KSI)			
LOCATION	Model w/ 30k	Testing w/ 30k	Model w/ 66k	Testing w/ 66k
Top-center of top continuity plate in bending	-0.855	-6	-1.88	-33
Vertical on the shear tab	-1.9	-8	-3.96	-81
Horizontal at top of shear tab	11.8	16	26.8	101
Horizontal at cope of shear tab	-2.6	-8	-5.7	-27

Analytical vs. Experimental Stresses for 1/2" Shear Tab (Session and Models 3)				
	STRESSES (KSI)			
LOCATION	Model w/ 30k	Testing w/ 30k	Model w/ 90k	Testing w/ 90k
Top-center of top continuity plate in bending	-1.11	-3	-3.33	-14
Top-center of top continuity plate in tension	0.3	0	0.93	8
Vertical on the shear tab	-0.63	-5	-2	-44
Horizontal at top of shear tab	12.7	10	38.2	81
Horizontal at cope of shear tab	-20.2	-10	-61.3	-67

Conclusions and Recommendations

Test and analytical results showed good qualitative agreement. The method outlined herein for designing extended shear tab connections of the type considered is more than adequate. For more definitive and detailed design guidelines, more data is needed through better analytical modeling and tests.

Detailed Design Example of an Extended Shear Tab

      The example below refers to the limit states discussed in chapter II. All stated equations and pages refer to the Manual. See Figure 62 for a sketch of the geometry of the design example.

DESIGN EXAMPLE GIVEN INFORMATION

Design Method:	LRFD
Weak axis beams (frame to column web):	W21x44 (Simple connection)
Strong axis beams (frame to column flanges):	W24x84 (Moment connection)
Column:	W14x99
Factored Reaction:	60 kips
Bolts:	A325-N ¾"-diameter
Distance "a" from toe of flange to bolt line:	2 ½ " to CL of bolts
Framing condition to column:	Square on CL
Bolt holes:	SSL in plate, STD in beam web
Hole horizontal edge distance:	1 ¾" from CL, 1 ¼ clear
Hole vertical edge distance:	1 ½" from CL, ~1 ⅛" clear
Hole vertical spacing:	3" center to center
Steel grades:	Plate A36; Rolled shapes A992

SOLUTION

    I.   Determine length of plate

    II.   Determine # of bolts and bolt configuration (m x n)

    III.   Check beam web thickness

    IV.   Determine thickness of plate

    V.   Determine weld locations and sizes
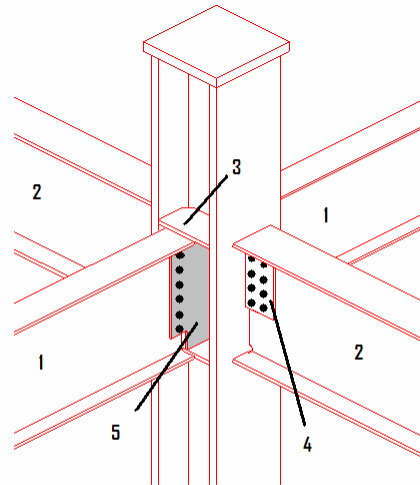
1. Beams that frame into the column web
2. Beams that frame into the column flanges
3. Top continuity plate for the moment connections
4. Standard shear tab for moment connection
5. Extended shear tab (to be analyzed)

Figure 62: The geometry of the design example

DETERMINE LENGTH OF PLATE

The length of the plate is readily found, as it is the clear distance between the continuity plates:

$$\text{Plate length} = d_{W24x84} - 2*tf_{W24x84} = 24.1 - 2*0.77 = \textbf{\underline{22.56"}}$$

DETERMINE # OF BOLTS AND BOLT CONFIGURATION   (Limit State A)

According to Table 7-10, each A-325N bolt in single shear can carry 15.9 kips.

In Table 7-17, the factored load is 60 kips and the design strength per bolt is 15.9 kips, so $C_{req} = 60/15.9 = 3.78$. Assuming the eccentricity from the load to the bolt line is 3", the table indicates that five bolts should be sufficient. In addition, five bolts will fit in one vertical row, so m x n = **5 x 1**. The factor C for five bolts is 3.9 and this gives a design strength of 3.9*15.9 = 62.01 kips.

CHECK BEAM WEB THICKNESS   (Limit State B)

The web thickness of a W21x44 is 0.35". With five bolts and an uncoped end condition, from Table 10-1 on page 10-26, the web strength is 439 kips/inch thickness. Since the thickness is only 0.35",

54

the strength of the beam web is 439 * 0.35 = 153 kips, which is greater than the end reaction of 60 kips, so

the beam web thickness is sufficient.

DETERMINE THICKNESS OF PLATE   (Limit States C-G)

It is initially assumed that the plate has a 3/8" thickness.   For other dimensions see Figure 63.
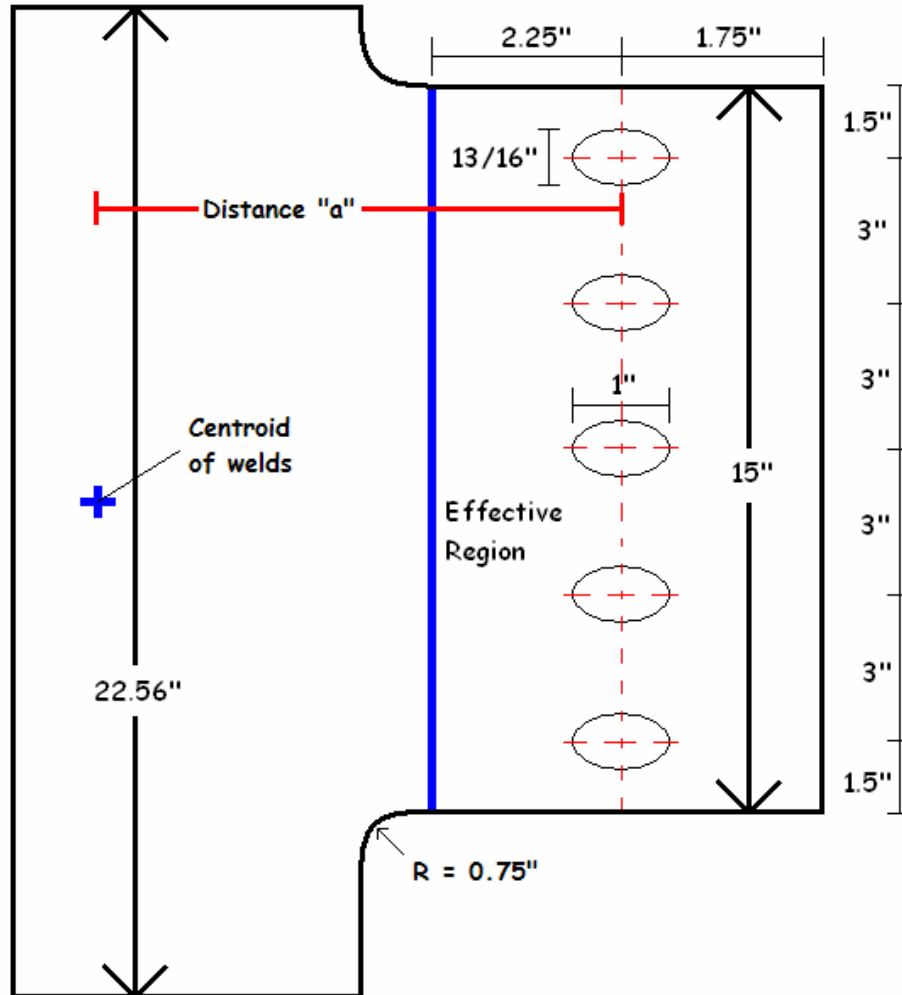
Figure 63: Overall dimensions of the extended shear tab

Check Shear Rupture:

Net Area for Shear A_{nv} = [15 − 5*(13/16)]*(3/8) = 4.10 sq. in.

Design Strength (Eq. J4-1) = 0.75*0.6*F_u*A_{nv} = 0.45*58*4.10 = 107 kips > 60 k   **OK**
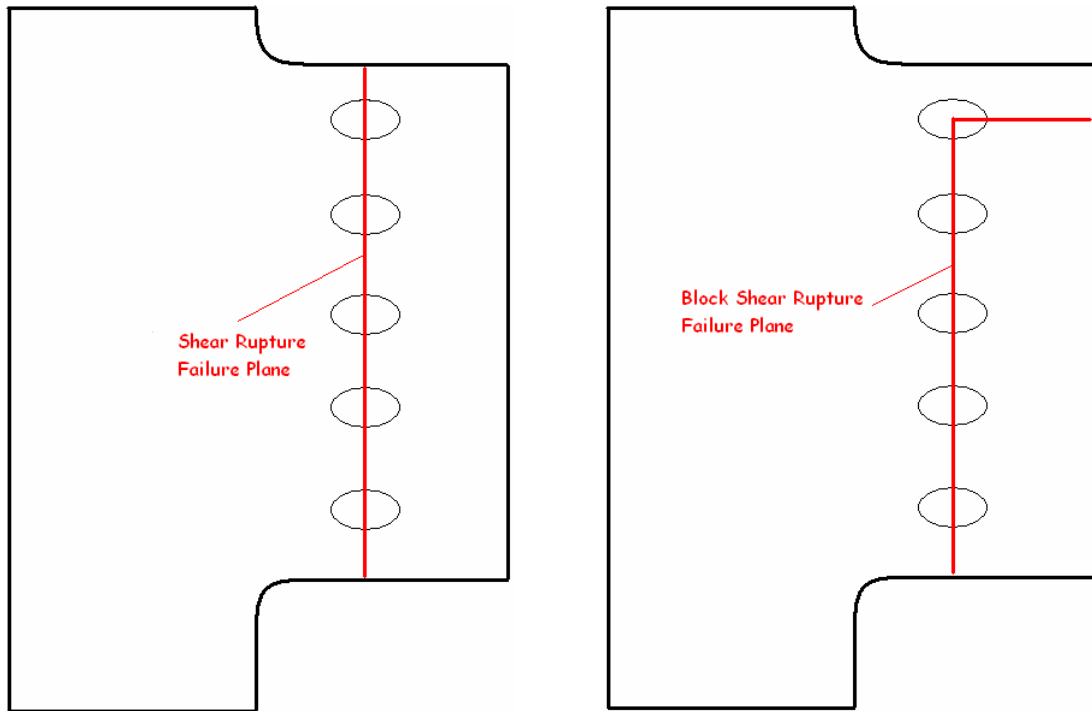
Figure 64: Failure planes for shear rupture and block shear rupture

Check Block Shear Rupture:

Net Area for Shear A_{nv} = [13.5 − 4.5*(13/16)]*(3/8) =   3.69   sq. in.

Net Area for Tension A_{nt} =   (1.75 − 0.5)*(3/8) =   0.46875 sq. in.

Gross Area for Shear A_{gv} = 13.5*(3/8) =   5.0625   sq. in.

Gross Area for Tension A_{gt} = 1.75*(3/8) =   0.65625 sq. in.

Check F_u*A_{nt} vs. 0.6*F_u*A_{nv} to determine which equation to use: 27.2 < 128.4   → Eq. J4-3b

Design strength = 0.75*[0.6*F_u*A_{nv} + F_y*A_{gt}] = 0.75*[0.6*58*3.69 + 36*0.65625] = 114 kips

Check to see if design strength exceeds the maximum design strength:

Max strength = 0.75*[0.6*F_u*A_{nv} + F_u*A_{nt}] = 0.75*[0.6*58*3.69 + 58*0.46875] = 117 kips

$$60k \ < \ 114 \, k \ < \ 117 \, k \quad \underline{\textbf{OK}}$$

The moment developed in the plate creates a tension-compression couple at the ends of the effective region of the plate. Due to the direction of the moment, the compressive force (C) acts horizontally at the bottom of the effective region of the plate and the tension force (T) acts horizontally at the top of the effective region. See Figure 65 for an illustration of the mechanics of the plate. The stress distribution of the plate is similar to that of a beam in bending, with a compression component at one end and a tension component at the other. The highest stresses in this case occur at the outer edges of the distribution. Therefore, it was determined that the distance of the couple is the distance between the outer edges of the stress distribution.
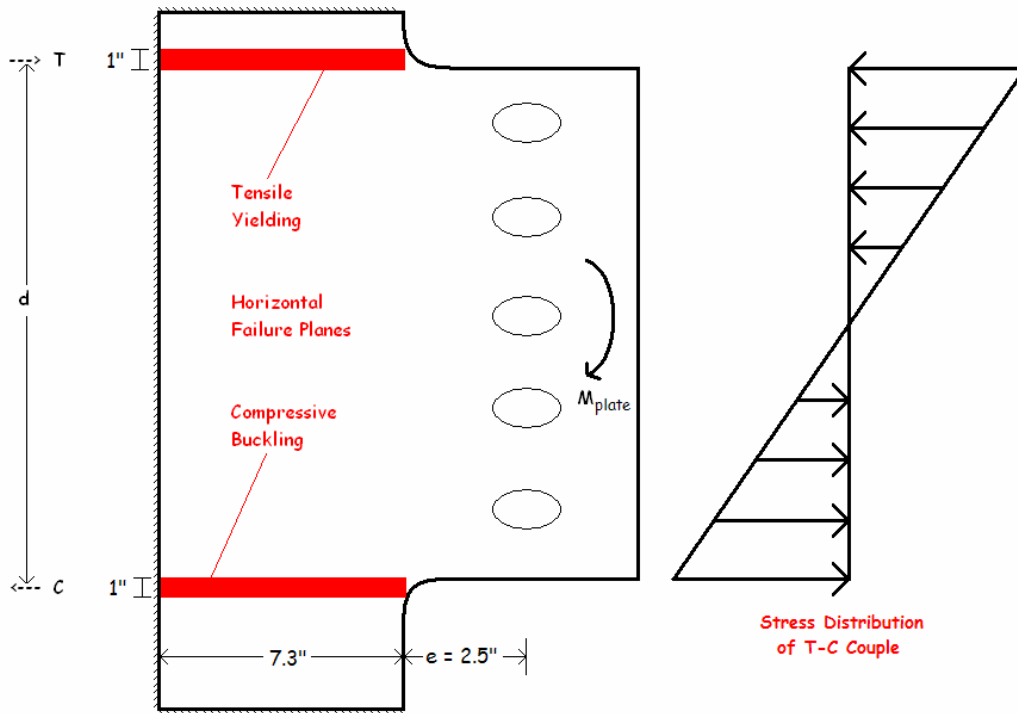
Figure 65: Horizontal failure planes due to the moment in the plate

In order to determine the resistant capacity of the plate against the T-C couple, an approximation was used. This approximation does not solve the particular mechanics of the problem, but it yields a safe design. Two horizontal strips of the plate are analyzed, one at each end of the effective region. One strip

resists compression, the other tension. The strength of the strip can then be extrapolated to a wider region of the plate.

Check Compressive Buckling Strip:

If the eccentricity is from the edge of the continuity plates to the bolts, then $e = 2.5$"

This gives a moment in the plate of 60 kips * 2.5" $= M_{plate} = 150$ k-in.

Since the T-C couple is $d = 15$" apart, $T = C = (150 \text{ k-in}) / (15 \text{ in}) = 10$ kips

The unbraced length of the column is 7.3".

One end is fully fixed and the other has rotation fixed, so the effective length factor $K = 1.2$ (p. 16.1-189).

The cross-section of the column is a 1" x (3/8)" rectangle.

Check width-thickness ratio (p. 16.1-14) $b/t = 1" / 0.375" = 2.67$

$$\lambda_r = 0.45*(E/F_y)^{0.5} = 12.8$$

$$\text{Since } b/t < \lambda_r, \text{ p. 16.1-27 can be used}$$

Analysis of the column from page 16.1-27:

λ_C $= (K*L/\pi/r)*(F_y/E)^{0.5}$ (Eq. E2-4)

A $= (1)(3/8) = 0.375$ sq. in.

I $= (1/12)*1*(3/8)^3 = 0.0044$ in.^{4}

r $= (I/A)^{0.5} = (0.0044/0.375)^{0.5} = 0.1083$"

λ_C $= (1.2*7.3/\pi/0.1083)*(36/29000)^{0.5} = (25.7)*(0.035) = 0.901$

F_{cr} $= 0.877*F_y/\lambda_C^2 = 0.877*36/0.901^2 = 38.9$ ksi   (Eq. E2-3)

Design strength (Eq. E2-1) $= 0.85*A*F_{cr}$

$= 0.85*0.375*38.9$

$= 12.4$ kips per inch strip

Considering the overall length of the plate is 22.56" and the effective length is 15", this is   **OK**

Check Horizontal Yielding:

The tensile force (T) that is acting is due to the moment in the plate caused by the eccentric loading. This occurs along a horizontal plane at the top of the effective region of the plate. From the previous moment analysis, T = 10 kips. This 10-kip tensile load acts horizontally in the region depicted in Figure 49. To determine the tensile strength of this region, a strip of 1-inch thickness is analyzed, which gives the strength per inch. Again, this strength can then be extrapolated to a wider region of the plate.

Analysis of the strip (Eqs. D1-1 and D1-2):

Since the effective area equals the gross area, yielding is the limit state that controls.

Design strength $= 0.9*F_y*A_g = 0.9*36*(1*(3/8)) = 12.15$ kips per inch strip $>$ 10 kips   **OK**

Check Bearing at Bolt Holes:

Design strength for each hole $= 0.75*1.2*L_c*t*F_u = 0.9*1.09*.375*58 =$ 21.4 kips

     $L_c = 1.5" - \frac{1}{2}(13/16") = 1.09375"$

Max design strength for each hole $= 0.75*2.4*d*t*F_u = 1.8*.75*.375*58 =$ 29.4 kips

So the bearing strength per hole is 21.4 kips.

With five holes, the overall bearing strength is 107 kips $>$ 60 k   **OK**

Check Shear Yielding of Plate:

Design strength $= 0.9*0.6*A_g*F_y = 0.9*0.6*(15" * 0.375")*36 = 109$ kips $>$ 60 k   **OK**

All of the critical limit states for the plate are OK

CHECK FLEXURAL STRENGTH OF CONTINUITY PLATES   (Limit State H)

The thickness of the continuity plates is determined by the flange size of the strong-axis beam. Since a W24x84 has a flange thickness of 0.77", the continuity plates are ¾" thick, which meets minimum requirements. The width and length are determined by the W14x99 column dimensions.

The length of the continuity plate is $d - 2*t_f = 14.2 - 2*0.78 =$ 12.64"

The width of the continuity plate is $(b_f - t_w)/2 = (14.6 - 0.485)/2 =$ 7.06"

The load of 60 kips is distributed among the six welds on the shear tab, four of which are transverse fillet welds that are 6.31" long while the other two are longitudinal fillet welds with a length of 15". So the length ratio of transverse weld to longitudinal weld is 25.24 : 30. Since transverse welds are roughly 1.5-times as strong as longitudinal welds, the transverse welds have a relative length of 37.86", giving a new ratio of 37.86 : 30. If the 60-kip load is distributed evenly among these 67.86" of weld, then the load per inch of weld is 0.884 kips. Since the longitudinal weld is to the column web, it is not considered in the design of the continuity plates. Thus, the load carried by the transverse welds (and thus the continuity plates) is: (37.86 inches) * (0.884 kips per inch) = 33.5 kips.

Since there are two continuity plates in support, the load is halved. The load per plate is 16.75 kips and this load is distributed uniformly over the 7.06" width.

Although each continuity plate is weld-supported along three edges, the strength will be checked assuming fixed supports at the two column flanges, a conservative approach ignoring the weld to the web of the column. Figure 66 shows one of the continuity plates under consideration acting as a beam.
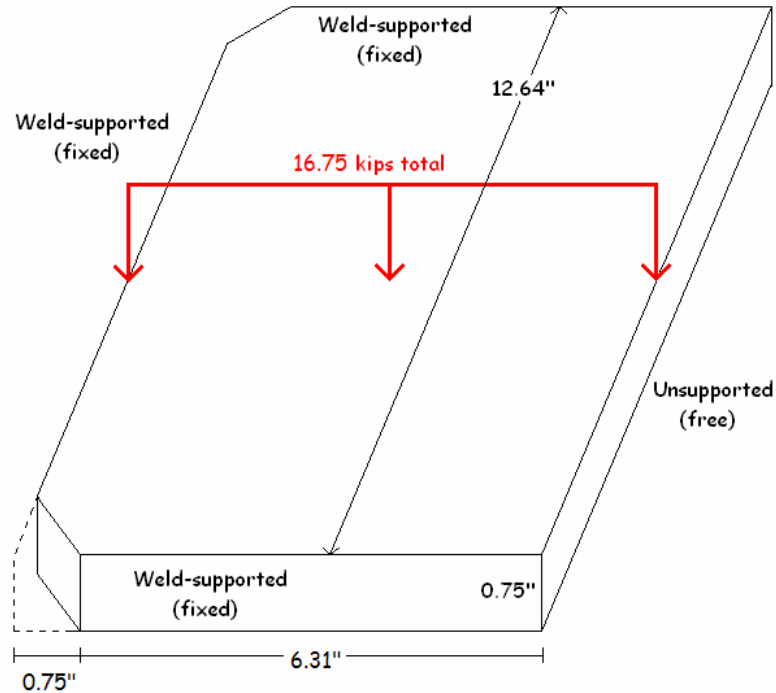
Figure 66: Flexural behavior of the continuity plate to stiffen the shear tab

Since the ends are fixed, the maximum moment developed at the centerline is less than that of a simply supported beam. The maximum moment, from page 5-167 of the Specification, is P*L/8 where P is 16.75 kips and L is 12.64". Therefore, the maximum moment is 26.5 k-in. The design strength (Eq. F1-1 of the Specification) of the "beam" is $\quad \Phi*M_n = \Phi*M_p = \Phi*1.5*M_y = \Phi*1.5*F_y*S_x$

where $F_y = 36$ ksi $\quad\quad \Phi = 0.9 \quad\quad S_x = (1/6)*b*d^2 = (1/6)*7.06*0.75^2 = 0.662$ in^3

So the flexural design strength of the "beam" is $\quad\quad \Phi*M_n = 32.2$ k-in $\quad > \quad 26.5$ k-in $\quad\quad$ **OK**

Without considering the weld along the column web, the continuity plates can support the load. Due to the added strength that the third weld would provide, continuing the design with ¾" plates is more than reasonable.

CHECK TENSILE STRENGTH OF CONTINUITY PLATES   (Limit State J)

The force acting in this case is the same as the force for horizontal yielding of the shear tab. See Figure 67 for an illustration of the failure mechanism.
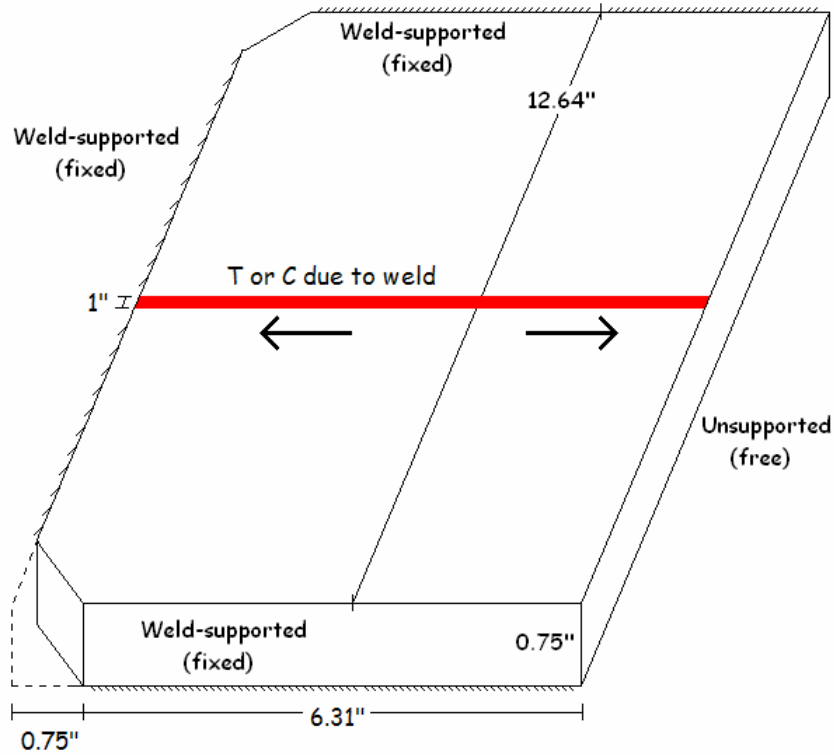
Figure 67: Tension and compression of the continuity plates caused by the weld from the shear tab

The load is $T = 10$ kips and there are two limit states to check. The design strength for yielding (Eq. D1-1) is $0.9*A_g*F_y$. The design strength for fracture (Eq. D1-2) is $0.75*A_e*F_u$. Analyzing a 1" strip of the plate, the area is a 1" x ¾" rectangle, so $A_g = 0.75$ in^2. The effective area equals the gross area so the controlling limit state is plate yielding.

The plate material is A36 so $\quad\quad F_y = 36$ ksi

For yielding, $\quad\quad 0.9*0.75*36 = 24.3$ kips > 10 kips $\quad\quad$ **OK**

CHECK COMPRESSIVE STRENGTH OF CONTINUITY PLATES (Limit State K)

The force acting is the same as above, except it is compressive, $C = 10$ kips. The continuity plate is considered to be a column with a length of 7.06". One end is fully fixed and the other is fixed against rotation, so the effective length factor from p. 16.1-189 is $K = 1.2$. The effective length of the column is 8.5". Analyzing a 1" strip of the column, the cross section is 1" wide by ¾" deep. See Figure 67 on the previous page again.

Check width-thickness ratio (p. 16.1-15) $\quad\quad b/t = 1" / 0.75" = 1.33$

$$\lambda_r = 1.49*(E/F_y)^{0.5} = 42.3$$

$$\text{Since } b/t < \lambda_r, \text{ p. 16.1-27 can be used}$$

Analysis of the column from page 16.1-27:

$\lambda_C \quad\quad = (K*L/\pi/r)*(F_y/E)^{0.5}$

$A \quad\quad = (1)(0.75) = 0.75$ sq. in.

$I \quad\quad = (1/12)*1*(0.75)^3 = 0.035$ in.^{4}

$r \quad\quad = (I/A)^{0.5} = (0.035/0.75)^{0.5} = 0.216"$

$\lambda_C \quad\quad = (1.2*7.06/\pi/0.216)*(36/29000)^{0.5} = (12.5)*(.035) = 0.437$

$F_{cr} \quad\quad = (0.658^{\wedge} \lambda_C{}^2)*F_y = 33.2$ ksi

Design strength $= 0.85*A*F_{cr} = 0.85*0.75*33.2 = 21.2$ kips > 10 kips $\quad\quad$ **OK**

DETERMINE WELD LOCATIONS AND SIZES (Limit State L)

The load on the welds is an eccentric load since it does not pass through the centroid of the welds. The effect of the eccentric load is a combined stress state of both torque and shear. There are 2 analysis

approaches for this situation, the elastic approach and the ultimate strength approach. For this problem, the Tables in the Manual are to be used to determine the strength of the weld pattern, and they utilize the ultimate strength approach for determining the capacity.

The geometry of the weld pattern is shown in Figure 68, along with the values to be used in Table 8-9 to find the coefficient C, which is necessary to design the weld thickness.

The vertical weld ℓ = 22.56"
The horizontal welds $k\ell$ = 7.06"
The center of gravity, c.g., is a distance $x\ell$ = 1.3589" from the vertical weld.
The eccentricity of the load to the c.g. of the weld is ex = 8.2"

k = 7.06 / 22.56 = 0.313

a = 8.2 / 22.56 = 0.3635

x = 1.3589 / 22.56 = 0.0602
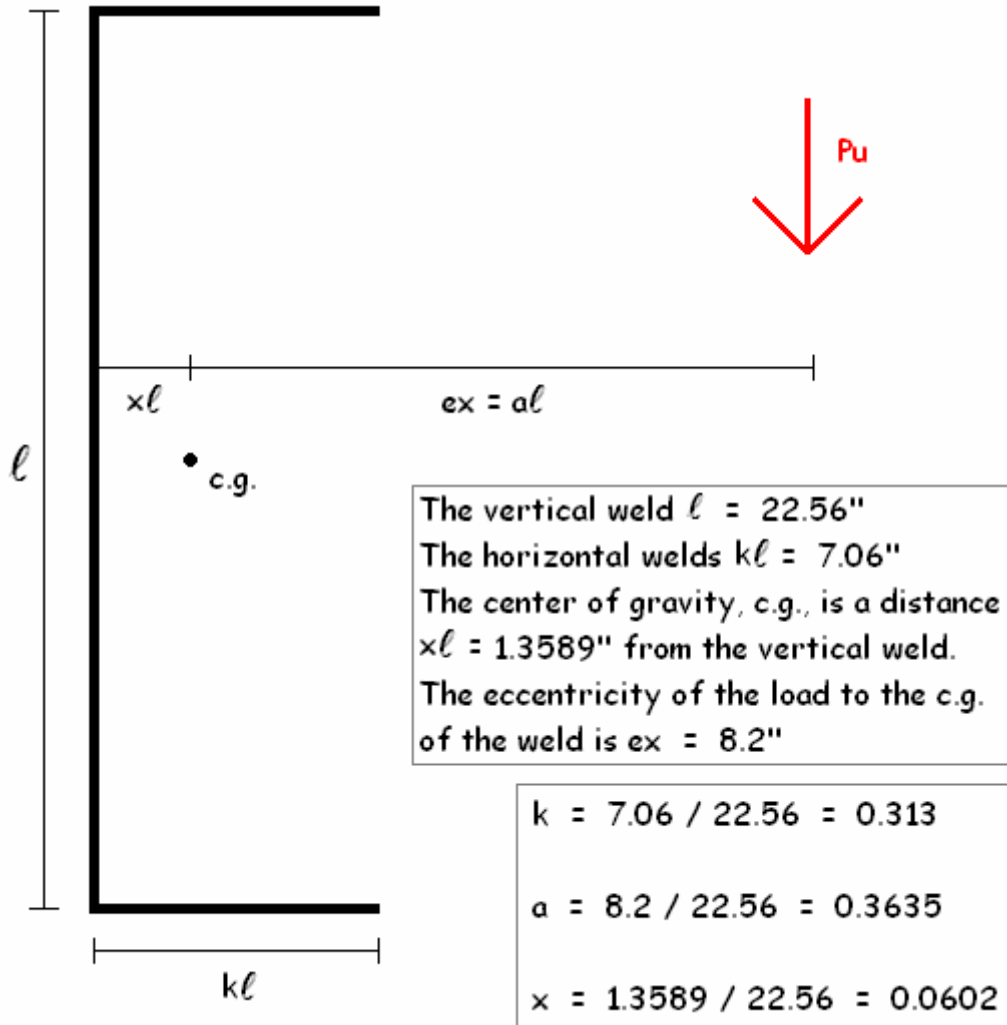
Figure 68: Geometry of the shear tab welds and values used to design the welds

For the welds, assume E70XX electrode, so from Table 8-4, C_1 = 1.00.

Interpolating from Table 8-9 with the given geometry, C = 1.97

D_{min} = the number of sixteenths of an inch in fillet weld size required to resist the load

D_{min} = $P_u/(C*C_1*l)$ = $(60) / (1.97*1.00*22.56)$ = 1.35

After rounding up to 2/16", the minimum weld size should be used. From Table J2.4 on page 16.1-54 of the Specification, the thicker material joined is the continuity plate, ¾". So in this case, the minimum fillet weld size is ¼". **¼" fillet weld should be used on both sides all the way around the shear tab.**

Loading Strategy for a Concentrated Load

     The most common type of loading in building design is a uniform load, so that on a beam it is distributed equally along the length of the member. Since a uniform load is difficult to achieve in a laboratory situation, the beam that was tested was not uniformly loaded, rather, it had one concentrated point load. However, an attempt was made to simulate the reaction and rotation of a uniformly loaded beam by placing the concentrated load at a predetermined location that would accomplish this. A typical uniformly loaded steel beam in a building may have a span of $L_1 = 25$ feet. For the tests in session 1, the length was $L_2 = 29$ feet. The calculations below show that the load needs to be placed approximately six feet from the support.

Uniformly loaded beam

End reaction, R_A
End rotation, θ_A

Point-loaded beam

End reaction, R_C
End rotation, θ_C
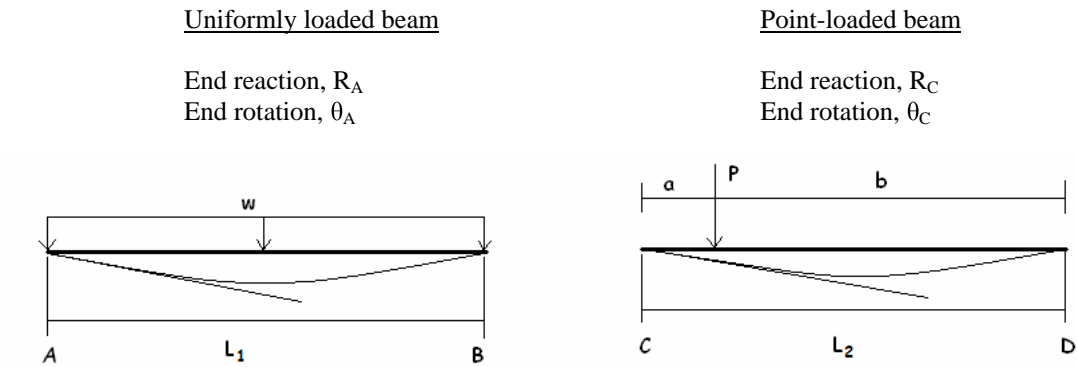
Figure 69: Diagrams used to determine the proper location of the concentrated load

$$R_A = \frac{w*L_1}{2}$$

$$\theta_A = \frac{w*(L_1)^3}{24E*I}$$

$$R_C = \frac{b*P}{L_2}$$

$$\theta_C = \frac{P*b*(L_2^2-b^2)}{6E*I*L_2}$$

     After solving R_A and θ_A for w, an expression of θ_A in terms of R_A can be found. Similarly, after solving R_C and θ_C for P, an expression of θ_C in terms of R_C can be found.

$$\theta_A \ = \ \frac{R_A*L_1{}^2}{12*E*I} \qquad\qquad\qquad \theta_C \ = \ \frac{R_C*(L_2{}^2-b^2)}{6*E*I}$$

Then, to get the same reaction and rotation, set the reactions equal to each other, $R_C = R_A$ and then solve $\theta_C = \theta_A$. The following expression is derived.

$$L_1{}^2 \ = \ 2*(L_2{}^2-b^2)$$

Using a typical $L_1 = 25$ feet and $L_2 = 29$ feet, $b = 23$ feet. This means that $a = 6$ feet, and this is the distance from the concentrated load to the support.

APPENDIX C

W27x84 Elasticity Analysis

To get consistent behavior from the same beam for all six tests, it was crucial to be sure that the beam remained elastic throughout all of the tests. Some localized plastic deformation was expected at the holes during the tests, but a six-inch end segment which included the holes was cut off each end of the beam after each session so that the ends of the beam were undamaged before the next session.

Some properties of a W27x84: T-dimension $= 23 \frac{5}{8}$"

Thickness of web $= 0.46$"

$S_{xx} = 213 \text{ in}^3$

- According to page 10-24 of the Manual, the strength of the beam web is 351 k/in for a 4-bolt connection. Similarly, the strength is 263 k/in for 3 bolts. Since the web thickness is 0.46", the strength of the web is 161 and 121 kips, respectively, which is sufficient for these tests.
  - o The beam web capacity is OK.
- The strength of the beam in flexure is taken from the Steel Beam Selection Tables. With an unbraced length of 15 feet, since it was braced at midspan, the flexural capacity is found on page 5-88 and is approximately 780 k-ft, which equals 9360 k-in. The maximum moment the beam experienced was at a reaction of 100 kips, so $M_{max} = (100 \text{ kips})*(6 \text{ feet}) = 7200$ k-in.
  - o The beam flexural capacity is OK.
  - o It should be noted that in test session 3, some lateral-torsional buckling was noticed. This most likely means that the plate system used to brace the beam at midspan did not provide a full brace at that point.

APPENDIX D

Sample Deflection and Rotation Calculation

For the test from session 1, in conjunction with #8 of Table 5-17 of the Manual, page 5-164

    a $= 6' = 72$"

    b $= 23' = 276$"

    L $= 29' = 348$"

    P $= 44.7$ kips

    E $= 29000$ ksi

    I $= 2850$ in^4 (W27x84)

$$\Delta_{max} = \frac{P*a*b*(a + 2b)*[(3a)(a + 2b)]^{0.5}}{27*E*I*L} = 0.26"$$

$$\Theta_{max} = \frac{P*b*(L^2 - b^2)}{6*L*E*I} = 0.0032 \text{ radians} = 0.184^o$$

APPENDIX E

Sample Shear Tab Design Using Table 10-9 of the Manual

Shear tab from test session 2 given information: 27.8-k factored end reaction

W14x99 column

W16x77 strong axis beam

See Figure 3 for a sketch of the configuration.

Overall length of shear tab $= d - 2t_f$ of W16x77 $= 16.5 - 2*0.76 = 14.98$"

Continuity plate thickness $= t_f$ of W16x77 $= 0.76$" say ¾"

From Table 10-9, page 10-120, use ¾" A325-N bolts and a flexible connection, so a ¼" plate with 3/16" fillet welds is sufficient, with a stated design capacity of 27.8 kips.

The continuity plate thickness is ¾" so the welds that fix the continuity plate to the column are 9/16". It is necessary to check these two sizes versus their minimum values, as stated in the proposed design procedure in Chapter III. The minimum size of the continuity plate is 1.5-times the thickness of the shear tab. Since the shear tab is only ¼" thick, the minimum is satisfied. The minimum size of the continuity plate-to-column welds is 1.5-times the thickness of the shear tab-to-continuity plate welds. Since these welds are only ¼", the minimum is satisfied.

In checking the minimum weld size to the ¾" continuity plates, the 3/16" fillet welds are insufficient. According to Table J2.4, page 16.1-54, the minimum weld size is ¼", which also requires the shear tab to be a 5/16" plate in Table 10-9. However, this minimum weld size was ignored and 3/16" fillet welds were used along with a ¼" shear tab, in an attempt to force the critical limit state onto the plate. The effective length of the shear tab $= 3$ holes $* 3$" c/c spacing $= 9$", which has to be greater than half the overall length of the tab, 14.98" / 2 $= 7.5$".

APPENDIX F

Detailed Procedure for Modeling Extended Shear Tabs in ANSYS

Steps in ANSYS analysis:

File – Clear and Start New – Do Not Read File – Yes (Execute Command)

File – Change Jobname

File – Change Title

Preferences – Structural – OK

Preprocessor – Element Type – Add – Add – Structural Mass Solid – Tet 10-Node 187 – OK – Close

Preprocessor – Material Properties – Material Models – Structural –

- For the elastic models, Linear – Elastic – Isotropic: EXY = 29000 ; PRXY = 0.31

- For the ultimate strength models, Linear – Elastic – Isotropic: EXY = 500 ; PRXY = 0.31

Preprocessor – Modeling – Create geometry using the following steps

- Create rectangle areas for the tall part of the tab and the extended part of tab

- Plot Ctrls – Window Controls – Window Options – Location of Triad – At bottom left

- Create keypoints for chamfered corners

- Create arbitrary areas through those keypoints

- Subtract the two arbitrary areas from the tall part of the tab and create the two arbitrary areas at the joints of the tall and extended parts of the tab

- Create circle areas in the extended part of tab (2 next to each other for each short-slotted hole), radius = 0.40625

- Create an arbitrary rectangle area through the keypoints of each circle to make the short slotted hole flat on top and bottom

- Subtract the three areas (2 circles and an arbitrary rectangle) of each short-slotted hole from the extended part of tab

- Glue the 4 areas together (2 rectangles and 2 chamfer triangles)

- Extrude each area along the normal by a distance equal to the thickness of the tab

70

- Plot Ctrls – Pan Zoom Rotate – Iso – Make sure everything looks right

- Create block volumes by dimension to add the continuity plates above and below the tab

- Glue all volumes together

Preprocessor – Meshing – MeshTool – SmartSize – 8 – Mesh – Pick All Volumes

List – Nodes – Coordinates Only – Sort First by X – Sort Second by Y – Sort Third by Z – OK – Save As NodeList.txt file

Solution – Define Loads – Apply – Structural – Displacement – On Areas – *SELECT* - All DOF Constant Value = 0

Solution – Define Loads – Apply – Structural – Pressure – On Areas – *SELECT* – Constant Value = …

Solution – Solve – Current LS – OK

General Postprocessor for results output:

- List Results – Nodal Solution – DOF Solution – All DOFs – Save As DOFList.txt file

- List Results – Nodal Solution – Stress – Components – Save As StressList.txt file

- Plot Results – Contour Plot – Nodal Solution – DOF Solution – UY – Print Screen – Save As DispY.bmp in MS Paint

- Plot Results – Contour Plot – Nodal Solution – Stress Solution – SX – Print Screen – Save As StressX.bmp

- Plot Results – Contour Plot – Nodal Solution – Stress Solution – SY – Print Screen – Save As StressY.bmp

- Plot Results – Contour Plot – Nodal Solution – Stress Solution – SZ – Print Screen – Save As StressZ.bmp

- Plot Results – Contour Plot – Nodal Solution – Stress Solution – SEQV – Print Screen – Save As StressVM.bmp

REFERENCES

AISC Manual of Steel Construction: Load and Resistance Factor Design. American Institute of Steel Construction, 3rd ed., 2001.

Allen, R.N. and J.W. Fisher, 1968, "Bolted Joints with Oversize or Slotted Holes," *Journal of the Structural Division*, Vol. 94, No. ST9, ASCE, Reston, VA.

Astaneh, A.,S.M. Call, and K.M. McMullin, 1989, "Design of Single-Plate Shear Connections," *Engineering Journal*, Vol. 26, No. 1, pp. 21-32, AISC, Chicago, IL.

ANSYS Verification Manual Release 5.3. ANSYS, Inc. 1996.

Bjorhovde, R., J. Brozzetti and A. Colson, 1988, *Connections in Steel Structures: Behaviour, Strength and Design*, Elsevier Applied Science, London, England.

Bjorhovde, R., J. Brozzetti and A. Colson, 1990, "Classification System for Beam-to-Column Connections," Journal *of Structural Engineering*, ASCE, Vol. 116, No. 11, pp. 3059-3076.

Bjorhovde, R., A. Colson, G. Haaijer, and J.W.B. Stark, 1992, *Connections in Steel Structures II: Behaviour, Strength and Design*, AISC, Chicago, IL.

Bjorhovde, R., A. Colson and R. Zandonini, 1996, *Connections in Steel Structures III: Behaviour, Strength and Design*, Pergamon Press, London, England.

Butler, L.J., S. Pal and G.L. Kulak, 1972, "Eccentrically Loaded Welded Connections," *Journal of the Structural Division*, Vol. 98, No. ST5, pp. 989-1005, ASCE, Reston, VA.

Ellifritt, D.S., and T. Sputo, 1999, "Design Criteria for Stiffened Seated Connections to Column Webs," *Engineering Journal*, Vol. 36, No. 4, pp. 160-167, AISC, Chicago, IL.

Ferrell, T.M., 2003, "Designing with Single Plate Connections," *Modern Steel Construction,* Vol. 43, No. 4, pp. 51-56.

Ferrell, T.M., D. Rutledge and C. Hewitt, "Preliminary Design Guide for Extended Shear Tabs". AISC and Ferrell Engineering Inc. Unpublished.

Fielding, D.J. and J.S. Huang, 1971, "Shear in Steel Beam-to-Column Connections," *Welding Journal*, AWS, Vol. 50, No. 7, Research Supplement, pp. 313-326.

Gaylord, E.H., C.N. Gaylord, and J.E. Stallmeyer, 1992, *Design of Steel Structures, 3rd Edition*, McGraw-Hill, Inc.

Higgins, T.R., 1971, "Treatment of Eccentrically Loaded Connections in the AISC Manual," *Engineering Journal*, Vol. 8, No. 2, pp. 52-54, AISC, Chicago, IL.

Huang, J.S., W.F. Chen, and L.S. Beedle, 1973, "Behavior and Design of Steel Beam-to-Column Moment Connections," *Bulletin 188*, October, Welding Research Council, New York, NY.

Nethercot, D.A., and W.F. Chen, 1988, "Effects of Connections on Columns," *Journal of Constructional Steel Research*, pp. 201-239, Elsevier Applied Science Publishers, Essex, England.

Research Council on Structural Connections, 2000, *Specification for Structural Joints Using ASTM A325 of A490 Bolts*, AISC, Chicago, IL.

Richard, R.M., D.E. Hormby and J.D. Kriegh, 1984, "Single-Plate Framing Connections with Grade-50 Steel and Composite Construction," *Engineering Journal*, Vol. 21, No. 3, AISC, Chicago, IL.

Richard, R.M., D.E. Hormby and J.D. Kriegh, 1982, "Design of Single Plate Framing Connections with A307 Bolts," *Engineering Journal*, Vol. 5, No. 4, AISC, Chicago, IL.

Salmon, C.G. and J.E. Johnson, 1996, *Steel Structures: Design and Behavior*, 4th ed., Harper Collins, New York, NY.

Sherman, D.R. and A. Ghorbanpoor, 2002, "Design Procedures for Extended Shear Tabs," Final Report Submitted to AISC, University of Wisconsin-Milwaukee.

Young, N.W. and R.O. Disque, 1981, "Design Aids for Single Plate Framing Connections," *Engineering Journal*, Vol. 18, No. 4, AISC, Chicago, IL.

http://computing.ee.ethz.ch/sepp/ansys-6.0-bo/ffcontact_tut.html#ffcont.15

http://www.aisc.org/Content/ContentGroups/Engineering_and_Research/Engineering_and_Research2/Teaching_Guide.pdf

https://pdc.usace.army.mil/ library/ufc/4-023-03/steel_reqs.pdf